GEOLOGICAL SURVEY OF CANADA

OPEN FILE 4088

Focal Mechanisms for Eastern Canadian Earthquakes: 1994-1995

A.L. Bent and H.K.C. Perry

2001

Natural Resources Canada Ressources naturelles Canada

Canada

FOCAL MECHANISMS FOR EASTERN CANADIAN EARTHQUAKES: 1994-1995

Allison L. Bent[1] and H. K. Claire Perry[2]

[1]National Earthquake Hazards Program
Geological Survey of Canada
7 Observatory Cres.
Ottawa, Ontario K1A 0Y3

[2]Dept. of Earth Sciences
University of Western Ontario
London, Ontario N6A 5B7

Geological Survey of Canada Open File 4088

August 2001
81 pp.

ABSTRACT

Although earthquake focal mechanism solutions provide information about the faults on which the earthquakes occur and on local stress field orientations and seismotectonics, they have not been routinely determined for eastern Canadian earthquakes. We have attempted to determine focal mechanisms for all eastern Canadian earthquakes of magnitude 4.0 or greater that occurred during 1994 and 1995. Of the ten earthquakes that met the selection criteria only one had a previously determined focal mechanism. We were able to obtain well-constrained focal mechanisms for five of the remaining nine events. The four for which solutions could not be determined occurred in the north where seismograph station coverage is poor. In this paper we summarize the solutions and tabulate all data used in their calculation.

RÉSUMÉ

Les mécanismes au foyer des tremblements de terre nous fournissent de l'information sur les failles sur lesquelles les tremblements de terre se produisent, et sur l'orientation des contraintes régionales et séismotectoniques mais on ne les détermine pas régulièrement dans l'est du Canada. Nous avons essayé de déterminer les mécanismes au foyer pour tous les tremblements de terre qui se sont produits dans l'est du Canada en 1994 et 1995 et de la magnitude 4,0 ou plus. Ces critères étaient satisfaits par dix tremblements de terre. Une solution de mécanisme au foyer existait pour un de ces séismes. On a déterminé les mécanismes au foyer pour cing des neuf autres tremblements de terre. On n'a pas pu obtenir des solutions pour quatre séismes qui se sont produits dans le nord où la couverture du réseau séismographique n'est pas suffisante. Dans cet article, nous faisons un sommaire des solutions et fournissons toutes les données que nous avons utilisées pour les déterminer.

INTRODUCTION

Earthquake focal mechanism solutions provide information about the faults on which the earthquakes occur and on local stress field orientations. If focal mechanisms can be determined for many earthquakes in a given region then we also gain insight into regional seismotectonic precesses and stress fields. In eastern Canada earthquake focal mechanisms are currently not routinely determined, although solutions may exist for individual earthquakes that were of particular interest as well as for some time periods or regions that have been systematically studied.

We have studied all eastern (roughly defined as east of 110° W) Canadian earthquakes of magnitude 4.0 or greater that occurred in 1994 and 1995 (Figs. 1 and 2) with the exception of those events for which focal mechanisms have been previously determined. Of the 10 events that matched the selection criteria, only one had a previously published focal mechanism. We were able to determine focal mechanisms for five of the remaining events. The four events for which we could not constrain the mechanism were small and occurred in the north where station coverage is sparse. However, in both cases, we were able to place some constraints on the stress axes.

Figure Captions:

Figure 1. Map of southeastern Canadian events studied. Symbol size is scaled to magnitude. Magnitude range 4.1-4.3.

Figure 2. Map of northeastern Canadian events studied. Symbol size is scaled to magnitude. Magnitude range 4.0-4.7.

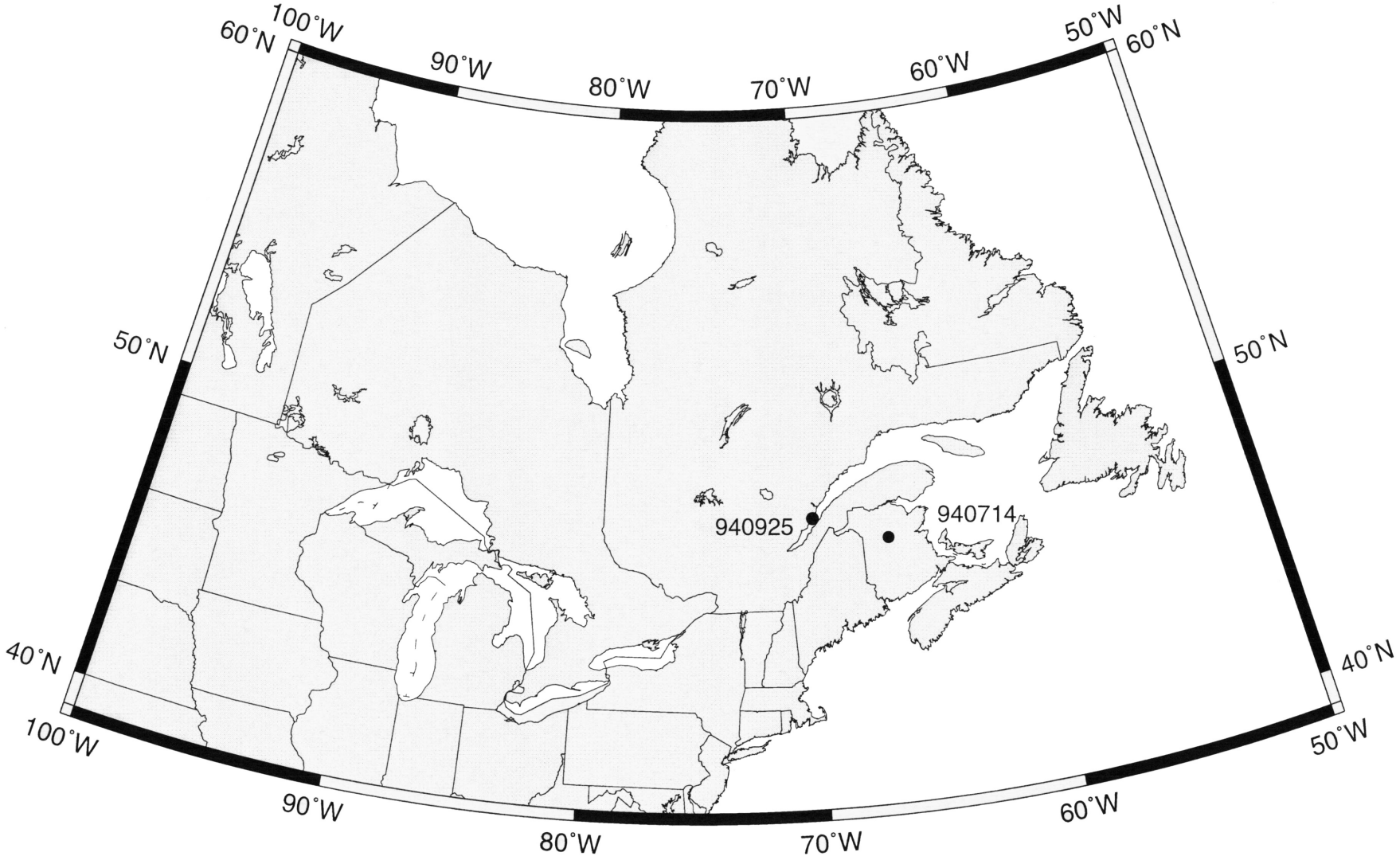
100°W
60°N
90°W
80°W
70°W
60°W
50°W
60°N
50°N
50°N
940925
940714
40°N
40°N
100°W
50°W
90°W
60°W
80°W
70°W

Figure 1

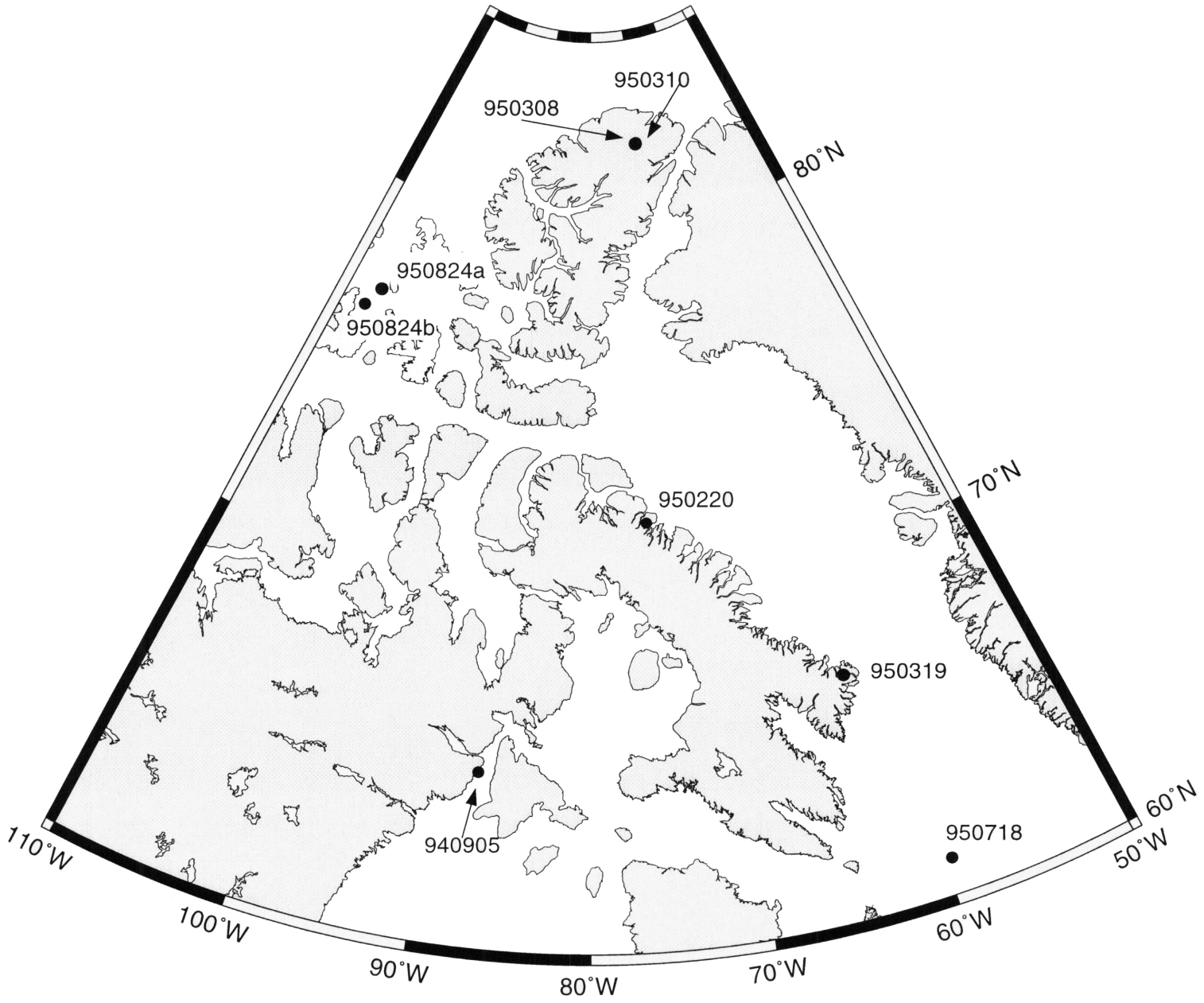
950310
950308
80°N
950824a
950824b
70°N
950220
950319
60°N
940905
950718
110°W
100°W
90°W
80°W
70°W
60°W
50°W

Figure 2

METHOD

The focal mechanisms were determined primarily from P wave first motions. We looked at the vertical component of all digital seismograms contained in the Canadian National Seismogram Network (CNSN; Fig. 3) optical disk archives in Ottawa. Both the continuously recorded data and the event files, which includes triggered data, were accessed. We also included any first motion data contained in the Canadian Earthquake Epicenter File (CEEF) database for which the seismograms were not archived. Generally these polarities were supplied by operators of regional networks or single stations within a few hundred kilometers of the epicenter. In the discussion of individual earthquakes, we note which polarities were not determined by the authors. We attempted to obtain additional seismograms or polarity data if they were likely to better constrain the solution, but did not routinely request external data for southern Canadian events. Similarly, we only attempted to read S polarities if the P data did not provide a well-constrained solution. For events from Baffin Bay to Ellesmere Island in the Arctic, we routinely requested data from two stations operated by the Incorporated Research Institutions for Seismology (IRIS) : Alert (ALE) on Ellesmere Island and Sondre Stromfjord (SFJ) on Greenland. Data from SFJ were also routinely requested for earthquakes in the Labrador Sea. For earthquakes occurring offshore along the southeastern margin, we consulted analog seismograms from stations in Guysborough, Nova Scotia (GBN) and St. John's, Newfoundland (STJN). For northern events we consulted the analog records from Igloolik, Northwest Territories (IGL). Most of the earthquakes we studied were relatively small (magnitude less than 5.0). Therefore, we did not routinely attempt to acquire teleseismic data. Locations of non-CNSN stations used in this study are shown in Figure 4. Unless explicitly stated otherwise, it should be assumed that any Canadian stations close to the epicenter from which polarity data are not noted were examined by the authors and that a first motion could not be determined.

Although we did not routinely search for seismogram data from non-Canadian stations at teleseismic distances, we checked the International Seismological Centre (ISC) bulletins for all events. We were able to obtain additional phase data for only one earthquake- the 8 March 1995 Ellesmere Island event.

We routinely read the polarities from unfiltered data. However, given that the earthquakes studied were generally small, it was occasionally necessary to filter some seismograms, particularly those from more distant broadband stations. Because high frequencies are attenuated more than low frequencies, there is always some danger that a first motion read from filtered data will not be the true first motion. By restricting the filtering of the broadband data to the frequency range of the short-period instruments, we should not adversely affect the data any more than most of instrument responses do. Unless stated otherwise, all filters were two-pole, single-pass Butterworth filters. Any filtering is noted on the seismogram traces where "hp" is used to designate a highpass filter, "lp" a lowpass filter and "bp" a bandpass filter. Corner frequencies are also noted. All filtering of data

was performed using the Seismic Analysis Code (SAC) routines (Tapley and Tull, 1991), which were also used to rotate horizontal records into their radial and tangential components.

The polarities were read independently by the authors. In case of disagreement, we re-examined the records in question. If a consensus was not reached, the polarity from that station was not used. If we agreed with respect sign, but one author read a polarity as impulsive and the other as emergent, the emergent polarity was retained.

As far as we have been able to ascertain the CNSN instrument polarities were correct during this time period. Polarities are usually checked once a year using a teleseismic event with a known focal mechanism.

The raw seismograms recorded by the CNSN are velocity records. Traditionally first motions have been read from displacement records. We looked at both velocity and displacement seismograms, using SAC to integrate the raw data.

To invert for the focal mechanism, the grid search algorithm of Snoke *et al.* (1984) was used. The search is based on the orientation of the B axis. Normal procedure was to initially search the focal sphere at 5° intervals. If no solutions were found to satisfy all the data, the search increment was gradually decreased. If with a 1° search no solutions were found, we returned to the 5° search, but allowed 1 polarity error. The procedure of alternately decreasing the search interval and increasing the the number of allowed polarity misfits was repeated until at least one solution was found. If the initial 5° no error search resulted in a large number of solutions or if there were large differences among the solutions, we attempted to find more polarity data by reading S wave polarities and/or looking for data from additional seismograph stations. For many of the offshore and northern events, the solutions could not always be further constrained.

If multiple but similar solutions were found for an earthquake, the preferred solution was selected by determining the mean strike, dip and rake and then selecting whichever of the actual solutions was closest to the mean. If multiple but dissimilar solutions were obtained for an earthquake, it was not always possible to obtain a preferred solution although conclusions regarding the stress axes orientations could sometimes be made.

We also note that the grid search algorithm ignores emergent first motions. In cases where the initial inversion resulted in large numbers of solutions or solutions which varied significantly from each other, we reran the program incorporating the emergent data. Emergent data were entered as impulsive and each impulsive polarity was entered twice, thereby giving them double weight. Any solutions obtained from weighted data are noted as such.

Earthquake epicenters were taken from the CEEF. With a few exceptions, depths for eastern Canadian earthquakes are fixed, usually at 18 km (roughly the midpoint of the crust). All nine of the events we studied had fixed depths although a calculated depth existed for the 1994 Charlevoix, Quebec earthquake,which had a previously published

focal mechanism solution. Since take-off angle is depth dependent, using an assumed depth will have some influence on the focal mechanism. Having said that, in most cases the effect will be minimal. As long as the hypocenter is within the crust, the take-off angle for Pn and teleseismic P will not be greatly influenced by the depth. At closer distances, the depth will have a greater effect on take-off angle and can also affect the Pg-Pn cross-over distance. However, the close stations are usually few in number, except in the Charlevoix region, where the depths are usually calculated. In any case, it is possible to determine how dependent the solution is on these stations by rerunning the grid search using take-off angles appropriate for various depths.

Figure Captions:

Figure 3. Map showing locations of CNSN stations in 1994-1995 from which polarity data were included in this study.

Figure 4. Map showing locations of non-CNSN stations from which polarity data were included in this study.

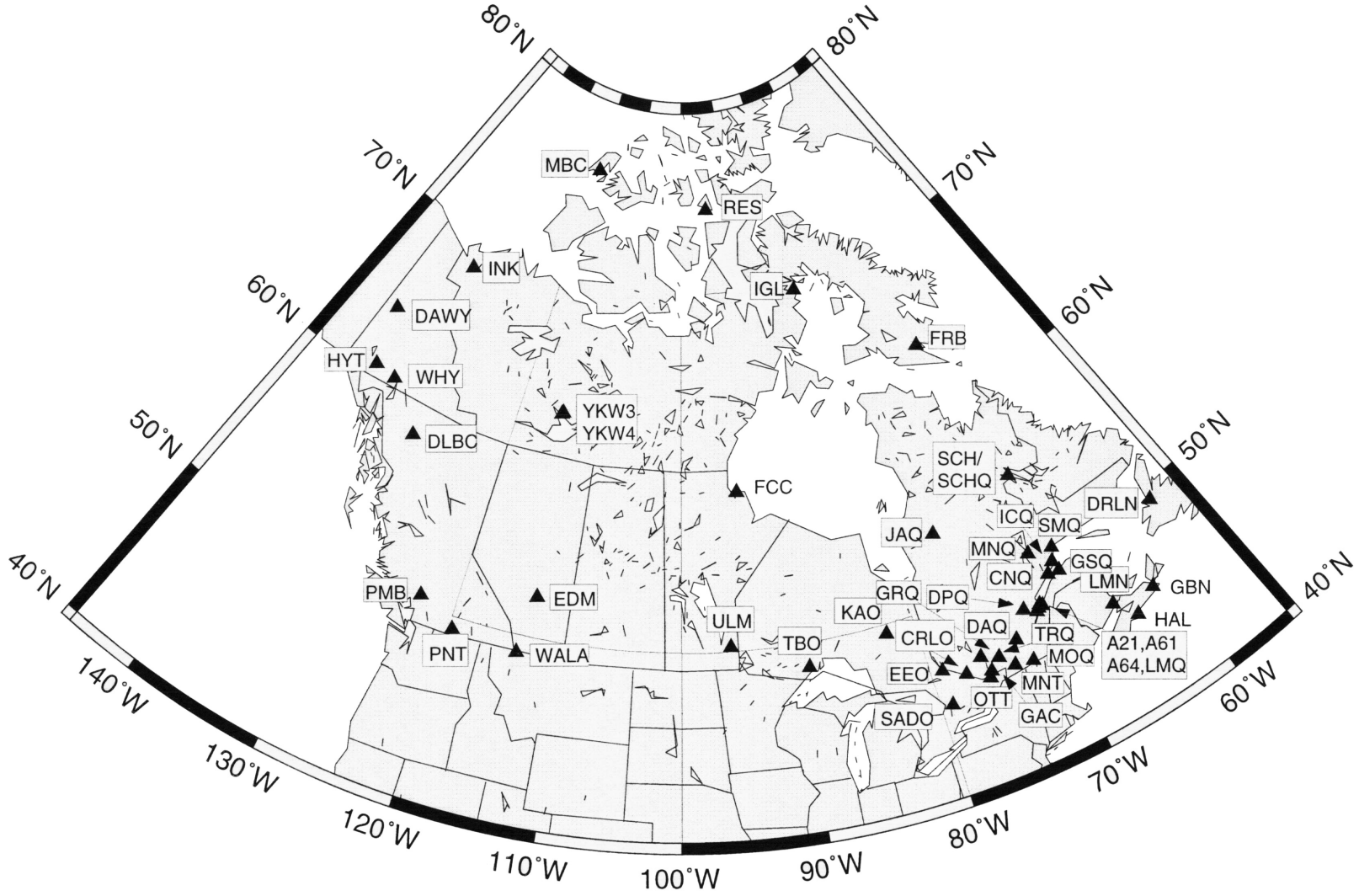
80°N
70°N
60°N
50°N
40°N
140°W
130°W
120°W
110°W
100°W
90°W
80°W
70°W
60°W
MBC
RES
INK
IGL
DAWY
FRB
HYT
WHY
YKW3
YKW4
DLBC
SCH/
SCHQ
FCC
DRLN
ICQ
SMQ
JAQ
MNQ
GSQ
CNQ
LMN
GBN
PMB
EDM
GRQ
DPQ
KAO
HAL
ULM
DAQ
TRQ
CRLO
A21,A61
A64,LMQ
PNT
WALA
TBO
MOQ
EEO
MNT
OTT
SADO
GAC

Figure 3

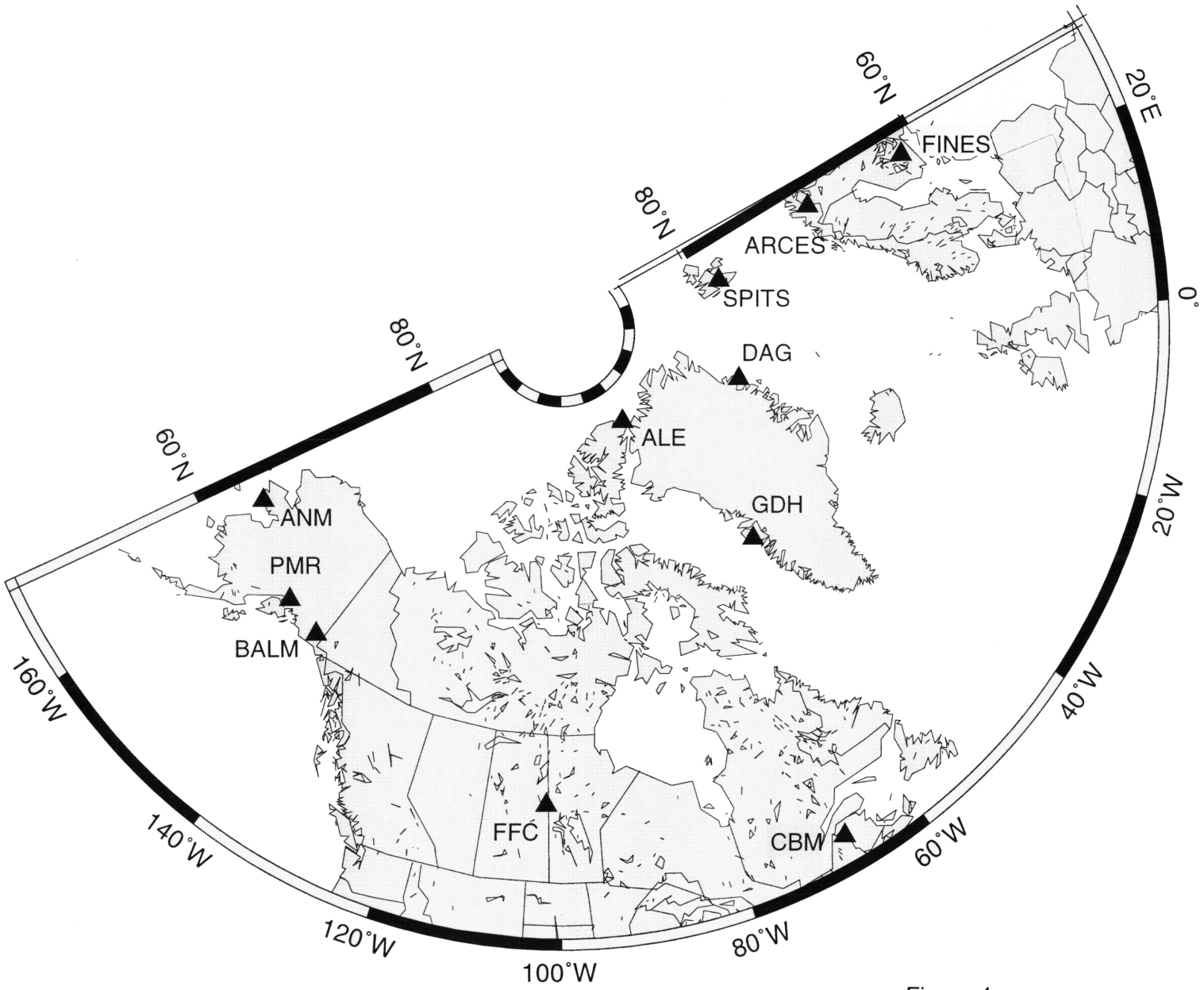
60°N
20°E
FINES
80°N
ARCES
SPITS
0°
80°N
DAG
ALE
60°N
GDH
20°W
ANM
PMR
BALM
160°W
40°W
FFC
CBM
140°W
60°W
120°W
80°W
100°W

Figure 4

FOCAL MECHANISMS

The epicenters for events included in this study are shown in Figures 1 (southeastern Canada) and 2 (northeastern Canada) and are identified by date of occurrence. For each earthquake, we include a list of polarities used to determine the fault plane solution(s). C's and D's indicate compressional and dilatational P polarities respectively. If the P polarity is emergent, a + indicates compression and a – indicates dilatation. SV waves are indicated by an F for motion toward the station or a B for motion toward the source. For SH waves, a < indicates counterclockwise motion (or to the left if one is facing the station with one's back to the source) and > indicates clockwise motion. Emergent S waves were not used as their polarities are difficult to pick with confidence. We also include portions of all digital seismograms from which we picked the first motions as well as focal mechanism solutions plotted in terms of both stress axes and P nodal planes.

In the seismogram figures that follow, the velocity records are shown. In an effort to be consistent, we have plotted a constant time window (4 sec) for each seismogram shown. This window is normally adequate to clearly illustrate the first motion, but we note that there may be occasions where showing a longer time segment or the displacement record might have provided stronger evidence for our choice of first motion.

All azimuths and strikes are measured in degrees clockwise from north. Take-off or incidence angles are measured from the vertical. Dip angles are measured from the horizontal. Rake is also known as slip angle. A rake of 0° implies pure left lateral strike-slip motion, 90° pure thrust motion, 180° pure right lateral strike-slip motion, and –90° (or 270°) pure normal faulting. Seismic source zones are as defined by Basham *et al.* (1982)

A quality factor of A, B, C, or D , with A being the highest quality, has been assigned to each focal mechanism determined. This factor should be taken not as a representation of how well the solution fits the data, but rather as an indication of how well constrained the solution is. Factors used to determine the quality include azimuthal coverage, number of first motions used and number of data points that do not fit the solution.

14 JULY 1994: MIRAMICHI, NEW BRUNSWICK

Seismic Zone:	Northern Appalachians
Latitude:	47.00° N
Longitude:	66.60° W
Depth:	5 km (fixed)
Magnitude:	4.1 (mN)
Origin Time:	12:41:52 (UT)
Comments:	felt in much of New Brunswick

Polarity Data

Station	Distance (km)	Azimuth (°)	Take-off Angle (°)	First Motion
CBM	116	267	–88.0	D
LMN	188	132	49.1	C
GSQ	216	350	49.0	D
CNQ	279	337	49.0	–
ICQ	285	350	49.0	–
LMQ	289	284	49.1	–
HAL	351	137	49.0	D
SMQ	359	359	49.0	C
DAQ	366	289	49.0	D
MNQ	424	339	49.0	C
GBN	431	112	49.0	C
DPQ	473	268	49.0	C
MOQ	476	249	49.0	D
MNT	567	255	49.0	C
GAC	698	261	49.1	D
SCH	871	359	49.1	C
EEO	952	272	49.1	C

Station	Distance (km)	Azimuth (°)	Take-off Angle (°)	First Motion
JAQ	996	323	49.0	D
SADO	1004	260	49.1	+
TBO	1712	285	49.1	–

Focal Mechanism Solutions

Strike	Dip	Rake
359.87	52.84	64.59
354.66	56.17	53.00
339.64	67.48	45.90
337.79	69.30	40.89
341.75	72.61	42.19
334.69	72.61	42.19
340.34	72.74	37.25
324.86	86.79	39.89
328.83	83.59	39.57
339.09	75.97	32.40
343.40	78.69	33.34
343.47	73.33	31.23
324.88	90.00	35.00
333.66	90.00	35.00
329.56	87.13	34.90
342.50	80.15	28.48
346.94	82.56	29.15
348.01	77.80	27.62
335.67	87.50	29.91

Strike	Dip	Rake
346.35	83.72	24.25
350.92	85.79	24.67
349.09	79.71	22.91
350.59	86.60	19.72
350.74	81.69	18.26

total number solutions: 24
grid search: 5°
misfits: 4
comments: CBM polarity provided by Weston Observatory; which stations misfit depends on solution; for preferred solution misfits at GAC, GBN, MNQ and MOQ

something wrong with stations GRQ, TRQ - all spikes

Preferred solution: use solution closest to mean

Plane 1:
- Strike: 343°
- Dip: 79°
- Rake: 33°

Plane 2:
- Strike: 246°
- Dip: 57°
- Rake: 167°

P-axis:
- Trend: 110°
- Plunge: 14°

T-axis:
- Trend: 210°
- Plunge: 31°

B-axis:
- Trend: 0°
- Plunge: 55°

Quality: A

good azimuthal coverage and redundancy; misfit stations are near-nodal; large number of observations

Figure Captions:

Figure 5a-e. Seismograms from which polarity data were read by the authors.

Figure 6. Focal mechanism solutions. Lower hemisphere projection. The P and T axes are shown on the left and the P nodal planes on the right. Data are also plotted. Solid symbols indicate compressional first motions and open symbols dilatations.

14 JULY 1994: MIRAMICHI, NEW BRUNSWICK

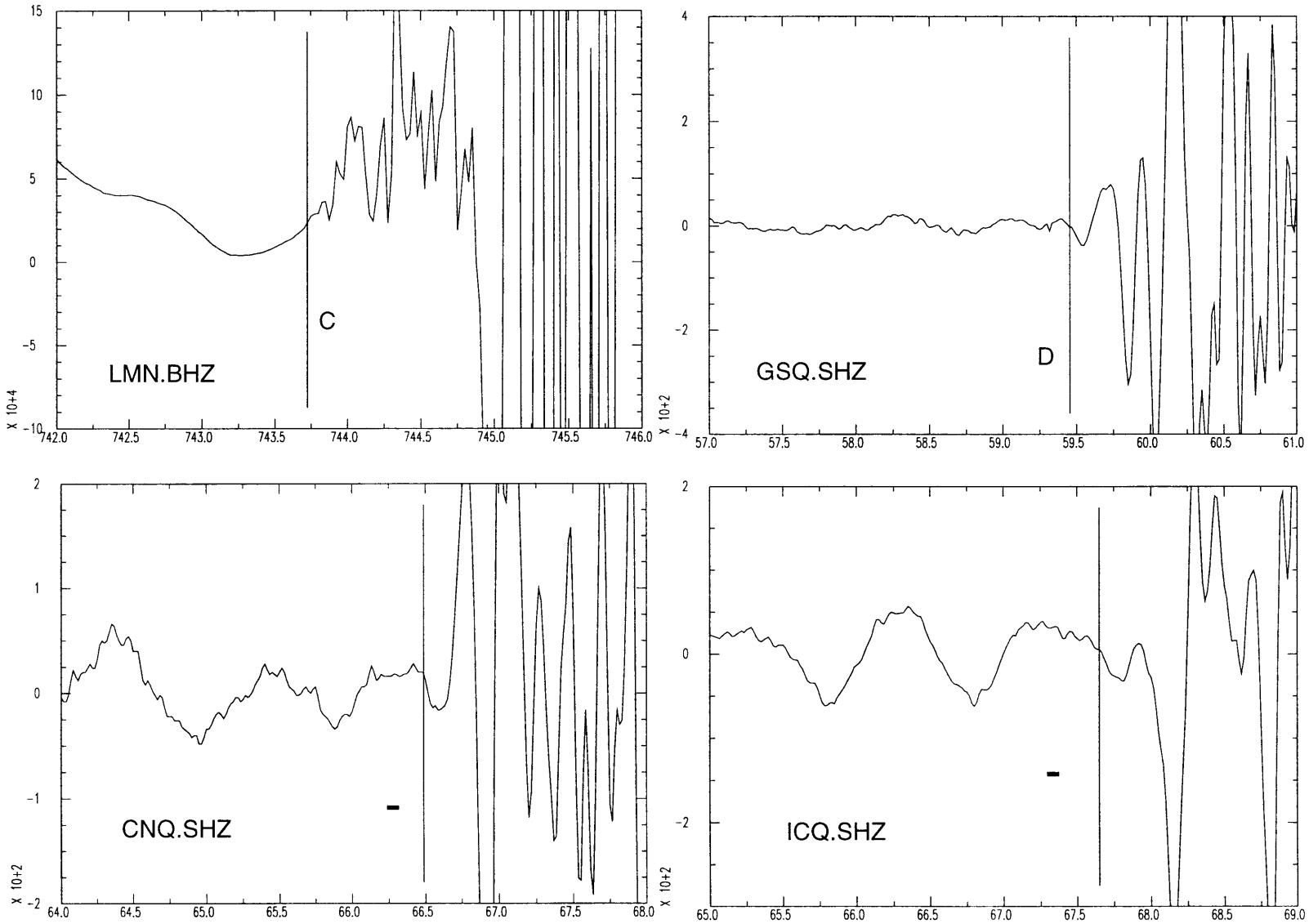

Figure 5a

14 JULY 1994: MIRAMICHI, NEW BRUNSWICK

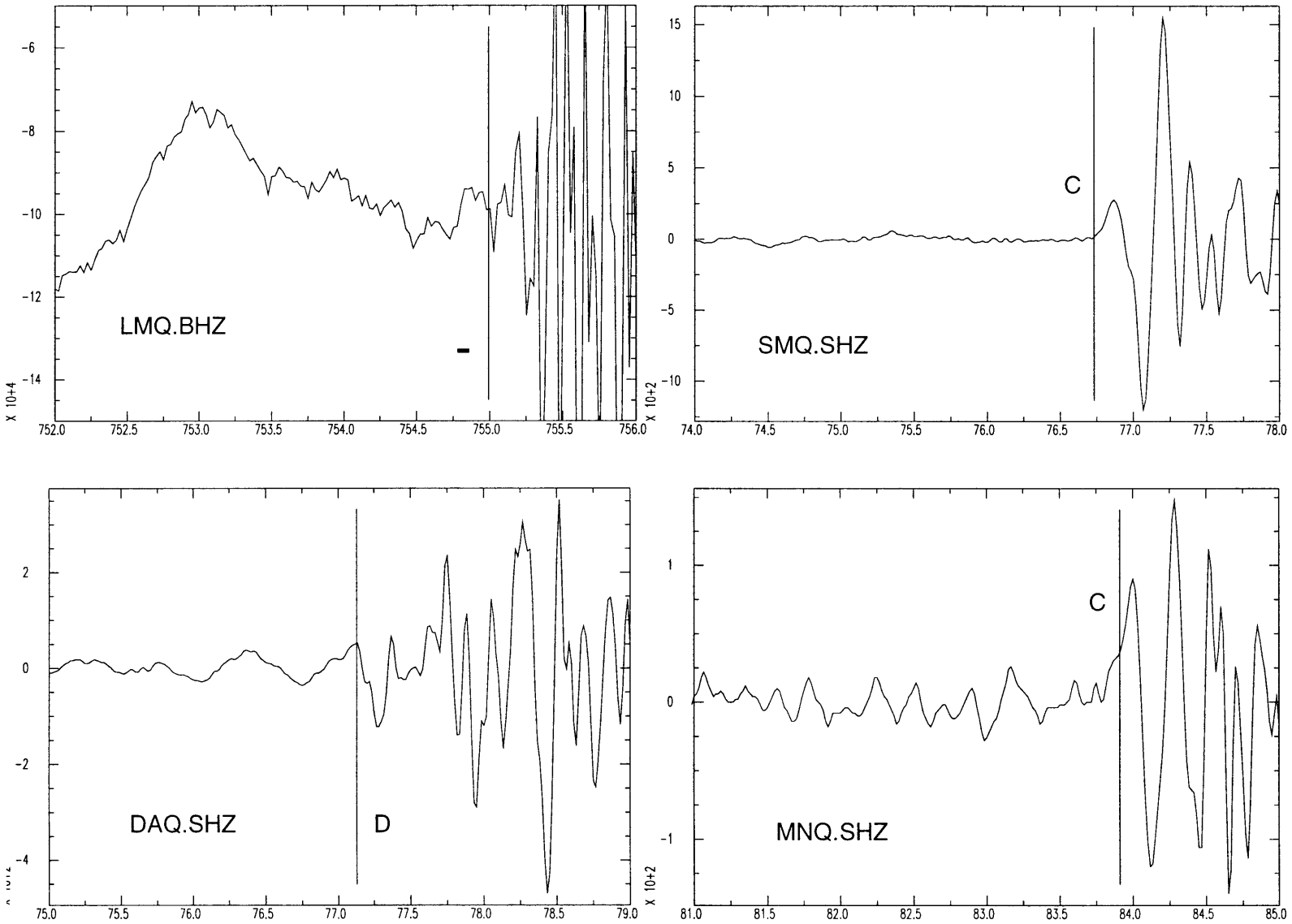

Figure 5b

14 JULY 1994: MIRAMICHI, NEW BRUNSWICK

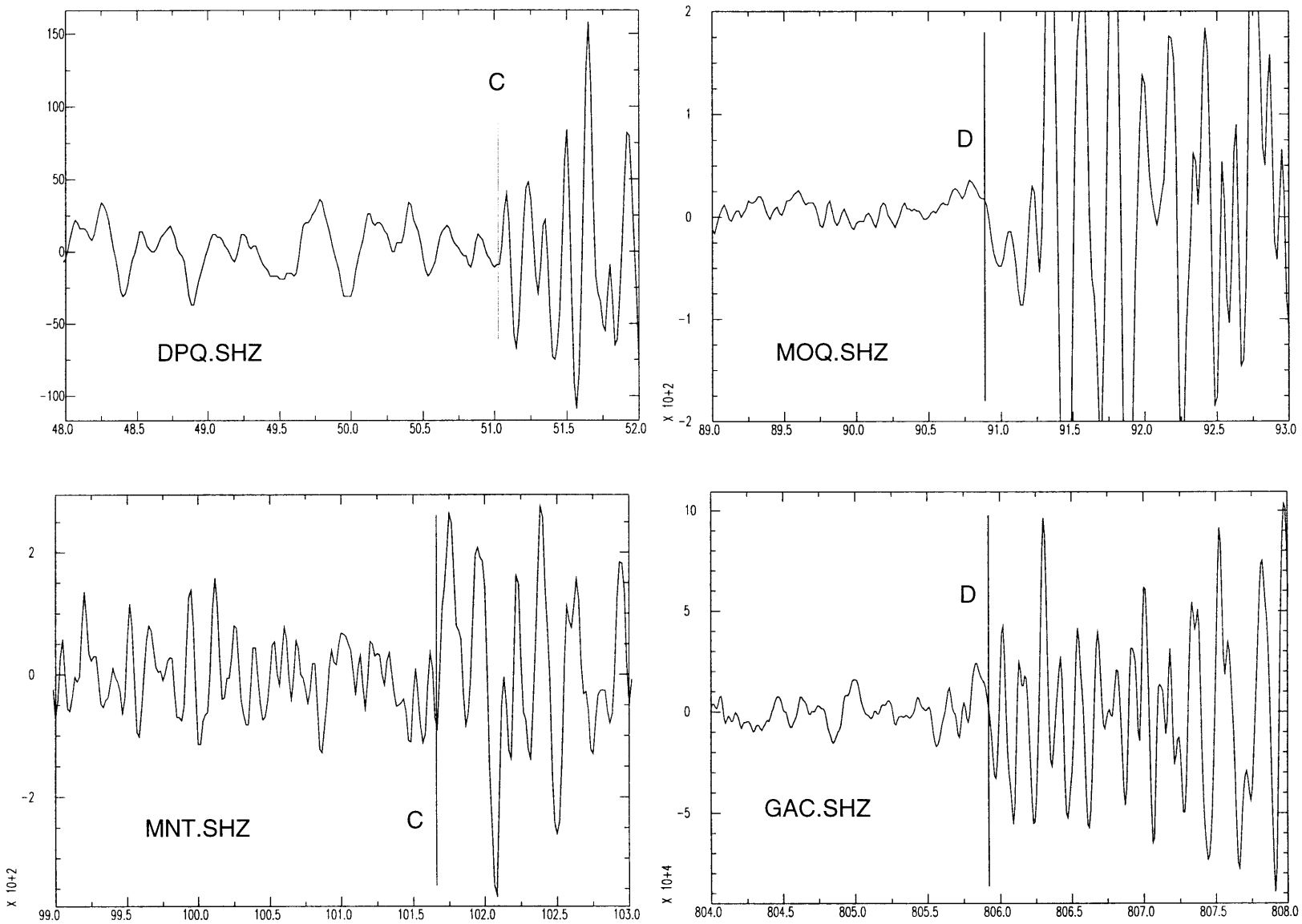

Figure 5c

14 JULY 1994: MIRAMICHI, NEW BRUNSWICK

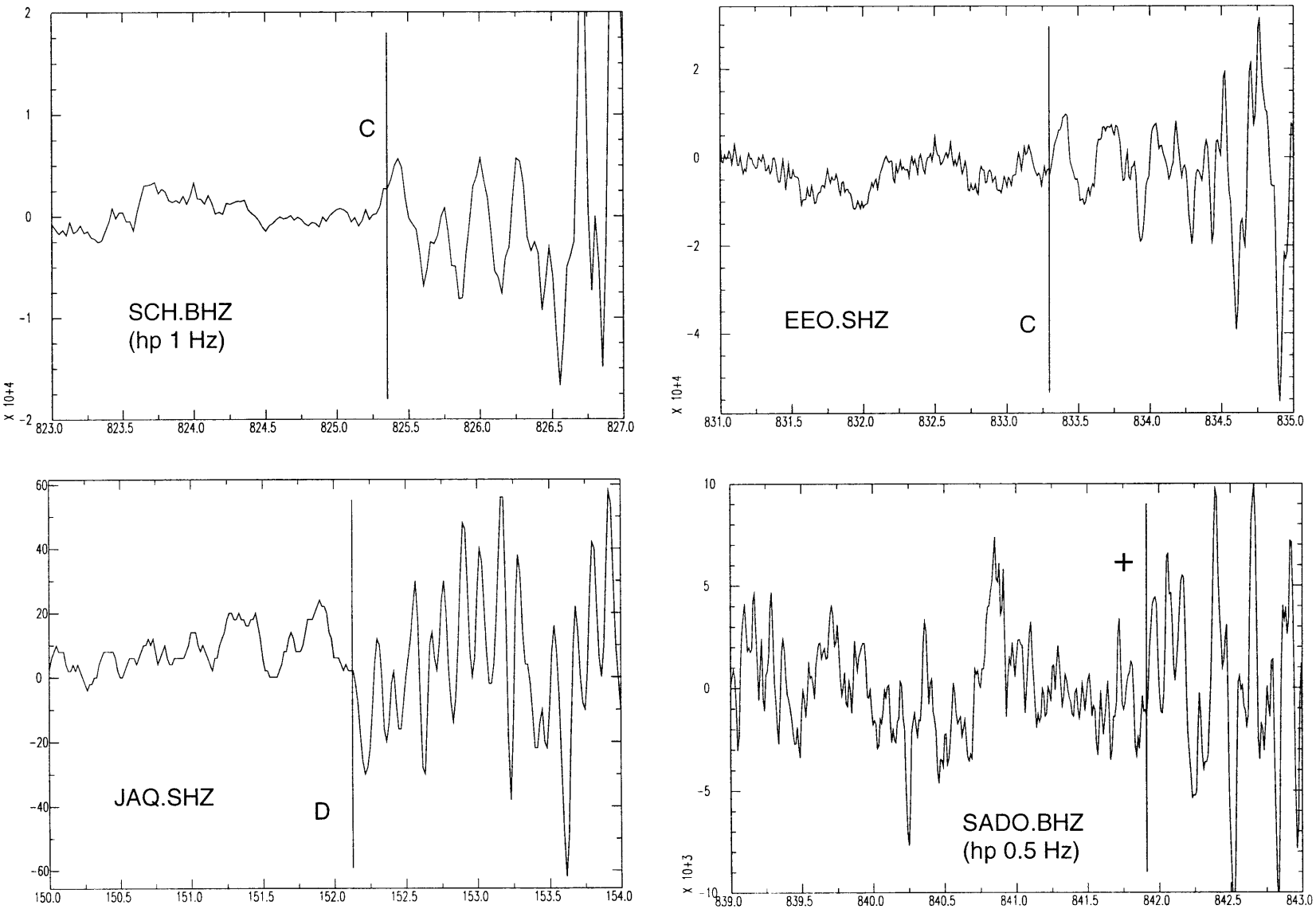

Figure 5d

14 JULY 1994: MIRAMICHI, NEW BRUNSWICK

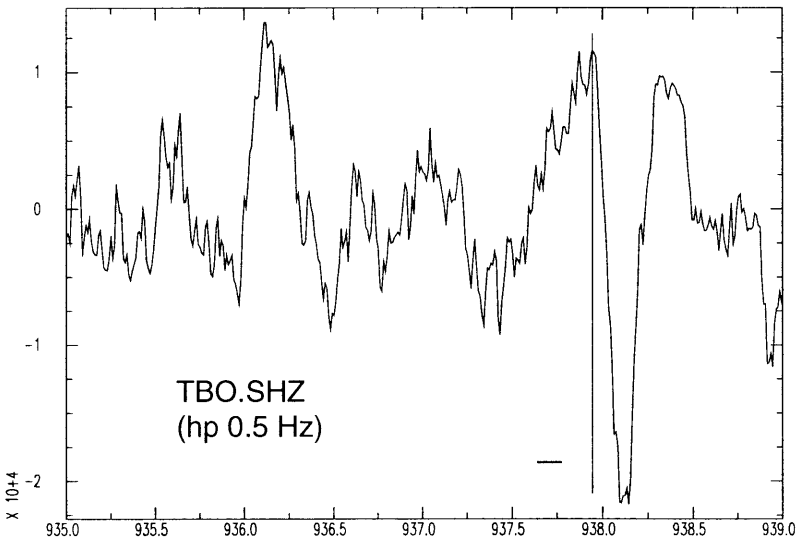

Figure 5e

MIRAMICHI, NEW BRUNSWICK: 14 JULY 1994

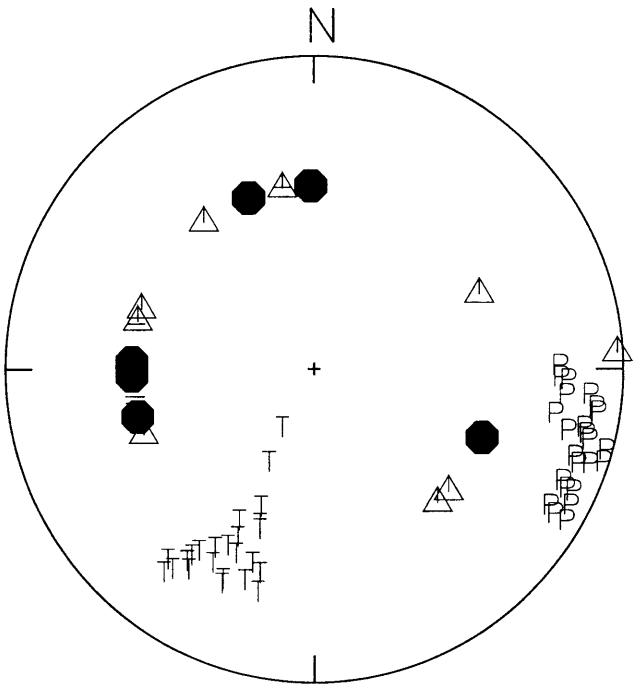

P and T axes

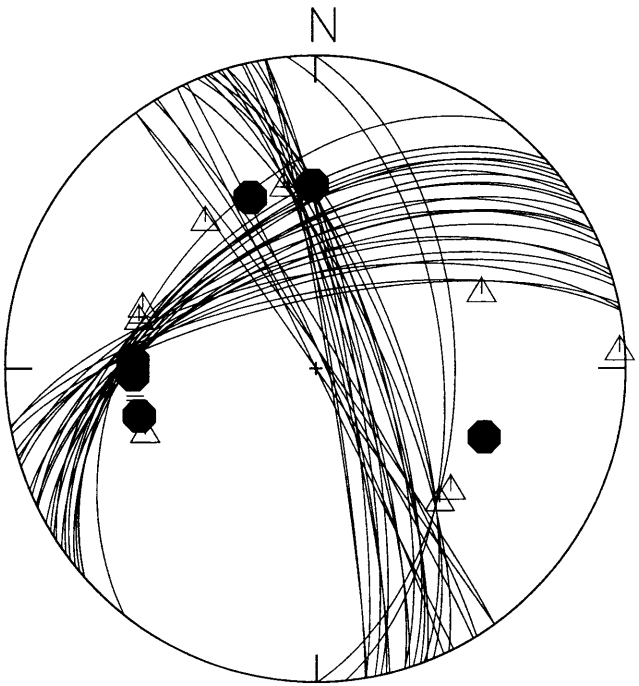

P nodal planes

Figure 6

5 SEPTEMBER 1994: ROES WELCOME SOUND, NWT

Seismic Zone: Boothia-Ungava
Latitude: 64.84° N
Longitude: 87.22° W
Depth: 18 km (fixed)
Magnitude: 4.3 (mN)
Origin Time: 22:51:09 (UT)
Comments:

Polarity Data

Station	Distance (km)	Azimuth (°)	Take-off Angle (°)	First Motion
FRB	910	89	49.0	-
RES	1138	348	49.0	-
SCH	1588	125	49.0	D
MBC	1706	331	49.0	D
KAO	1738	168	49.0	C
DRLN	2463	121	39.00	D

Focal Mechanism Solutions

total number solutions: 1396
grid search: 5°
misfits: 0
comments:

Preferred solution:

Nodal Planes:
Strike: insufficient data to determine
Dip: insufficient data to determine
Rake: insufficient data to determine

P-axis:		
	Trend:	NW-SE or NE quadrant
	Plunge:	shallow if NW-SE, moderate to steep if NE
T-axis:		
	Trend:	SW quadrant, a few solutions NE
	Plunge:	insufficient data to determine
B-axis:		
	Trend:	not in SW quadrant
	Plunge:	insufficient data to determine

Figure Captions:

Figure 7a-b. Digital seismograms from which polarity data were read by the authors.

Figure 8. Focal mechanism solutions. Lower hemisphere projection. The P axes are shown on the left and the T axes on the right. Data are also plotted. Solid symbols indicate compressional first motions and open symbols dilatations.

5 SEPTEMBER 1994: ROES WELCOME SOUND, NORTHWEST TERRITORIES

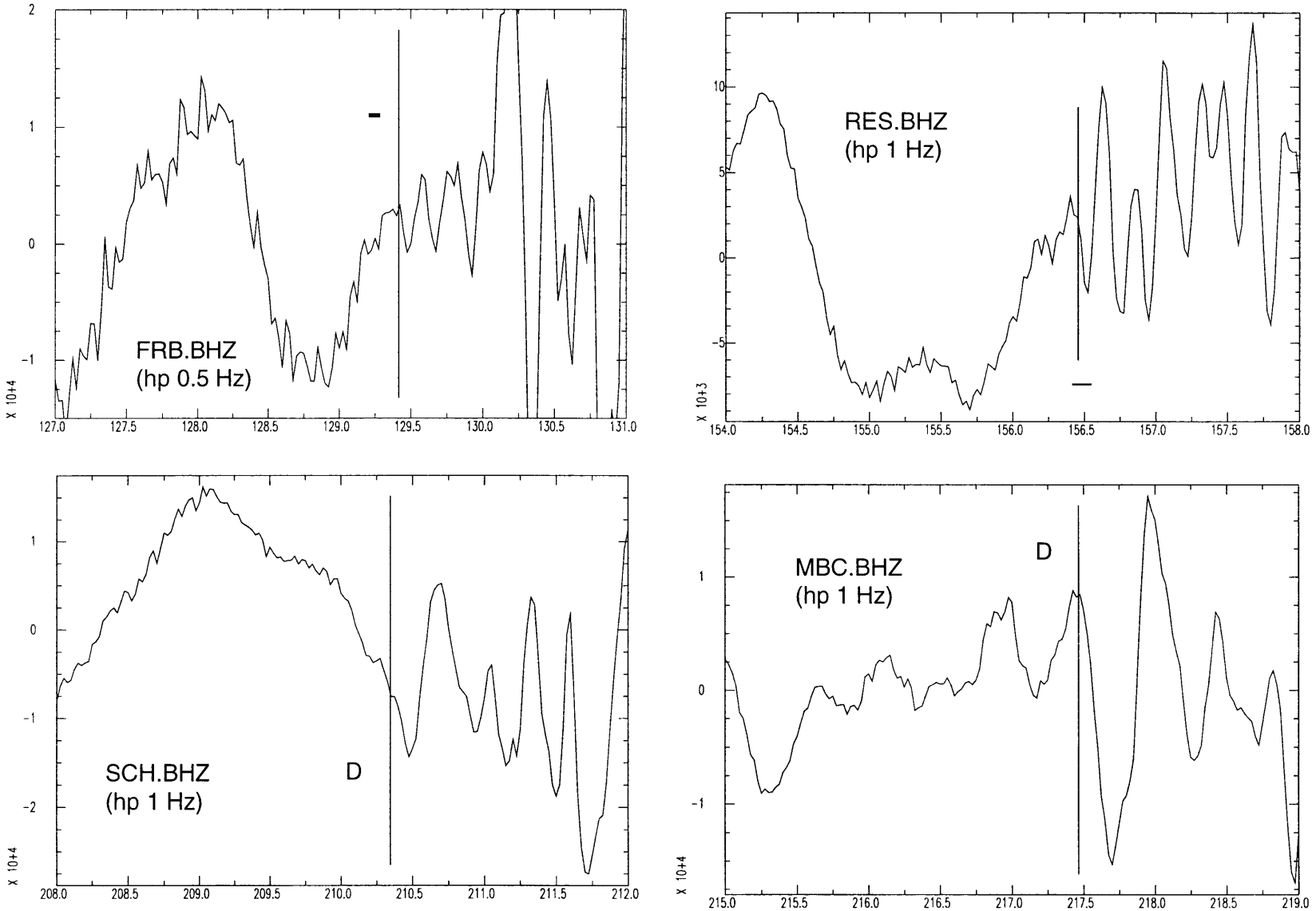

Figure 7a

5 SEPTEMBER 1994: ROES WELCOME SOUND, NORTHWEST TERRITORIES

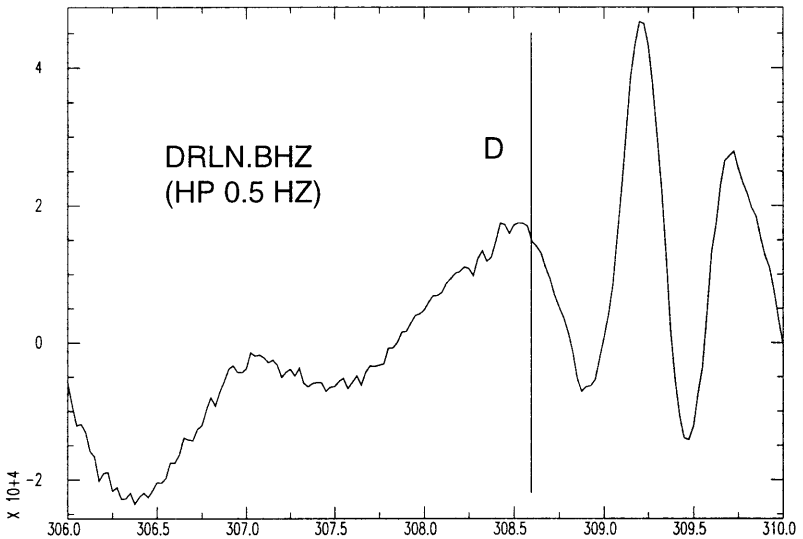

Figure 7b

5 SEPTEMBER 1994: ROES WELCOME SOUND, NORTHWEST TERRITORIES

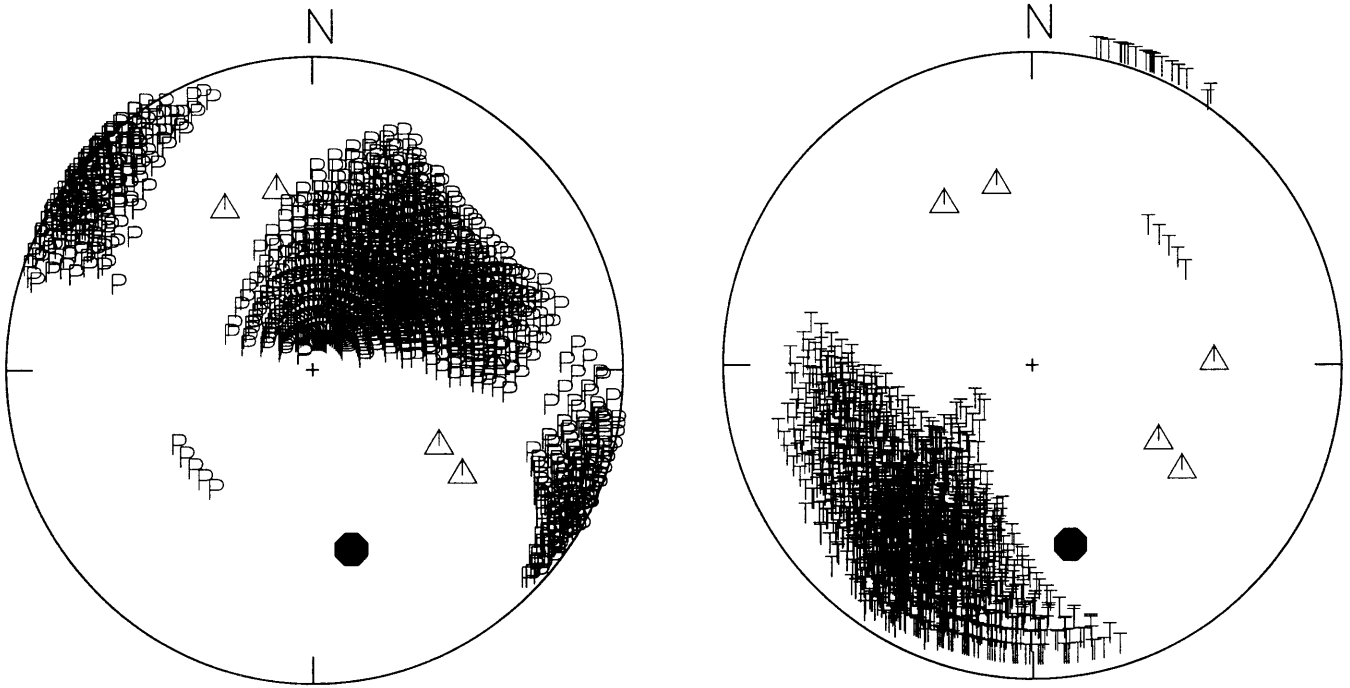

P axes

T axes

Figure 8

20 FEBRUARY 1995: BAFFIN ISLAND, NORTHWEST TERRITORIES

Seismic Zone: Baffin Island
Latitude: 71.82° N
Longitude: 75.10° W
Depth: 18 km (fixed)
Magnitude: 4.0 (mN)
Origin Time: 04:37:26 (UT)
Comments:

Polarity Data

Station	Distance (km)	Azimuth (°)	Take-off Angle (°)	First Motion
IGL	370	226	49.1	C
RES	709	306	49.1	D
FRB	942	160	49.1	D
MBC	1408	310	49.1	D
FCC	1690	220	49.1	C

Focal Mechanism Solutions

total number solutions: 285
grid search: 5°
misfits: 0
comments:

Preferred solution:

Nodal planes:
Strike: insufficient data to determine
Dip: insufficient data to determine
Rake: insufficient data to determine
P-axis:
Trend: NW-SE
Plunge: insufficient data to determine
T-axis:
Trend: NE-SW
Plunge: probably shallow (but not required to be)

B-axis:
Trend: insufficient data to determine
Plunge:insufficient data to determine

Figure Captions:

Figure 9. Digital seismograms from which polarity data were read by the authors.

Figure 10. Focal mechanism solutions. Lower hemisphere projection. The P and T axes are shown on the left and the P nodal planes on the right. Data are also plotted. Solid symbols indicate compressional first motions and open symbols dilatations.

20 FEBRUARY 1995: BAFFIN ISLAND, NORTHWEST TERRITORIES

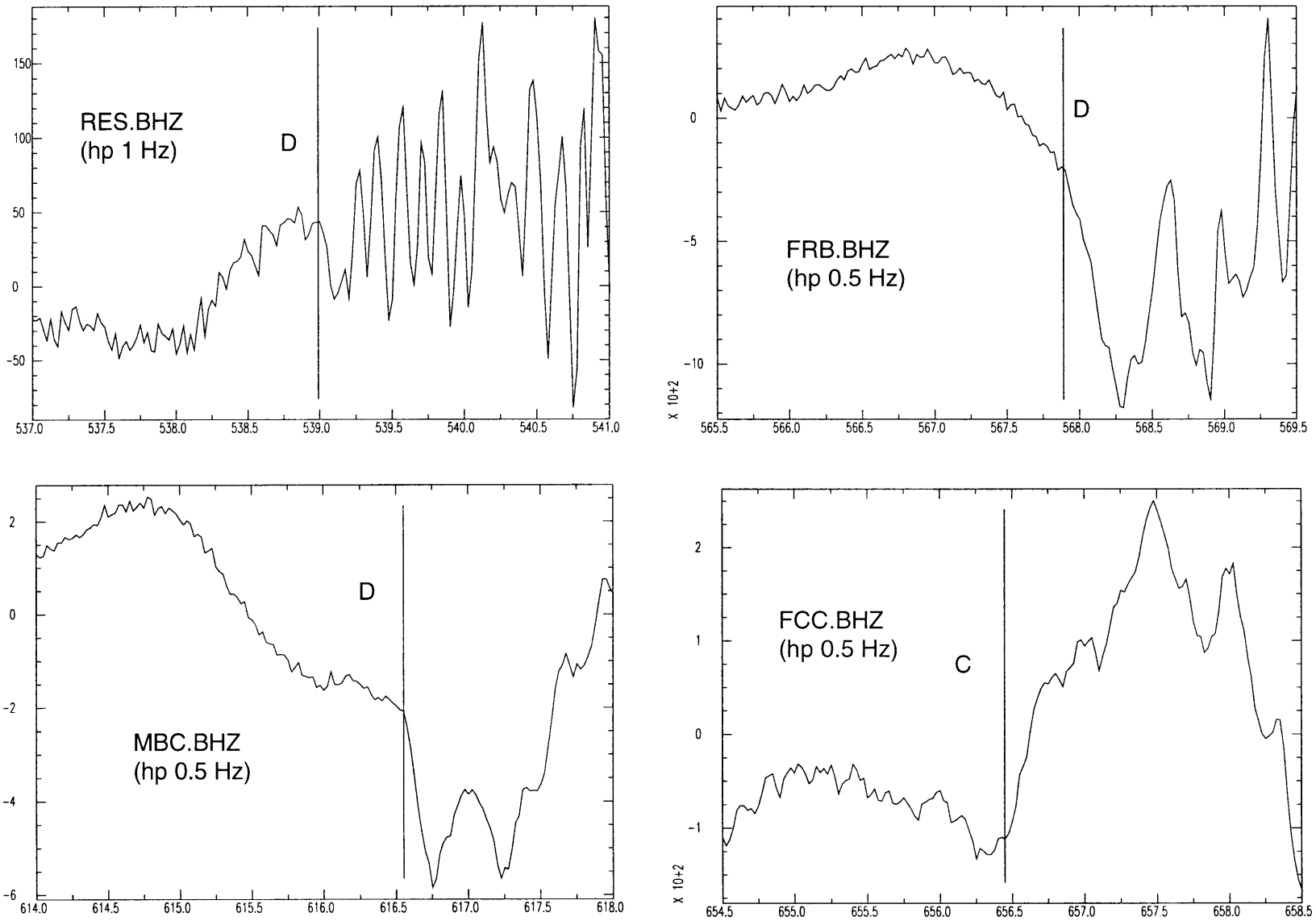

Figure 9

BAFFIN ISLAND, NORTHWEST TERRITORIES: 20 FEBRUARY 1995

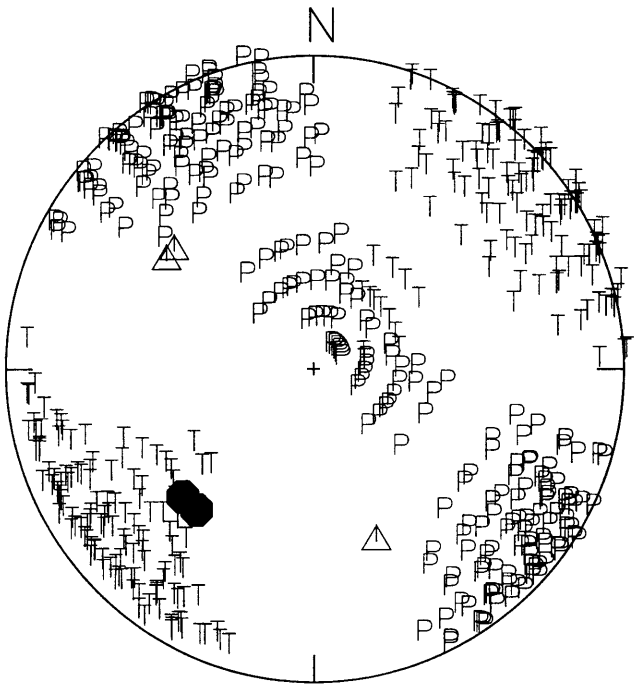

P and T axes

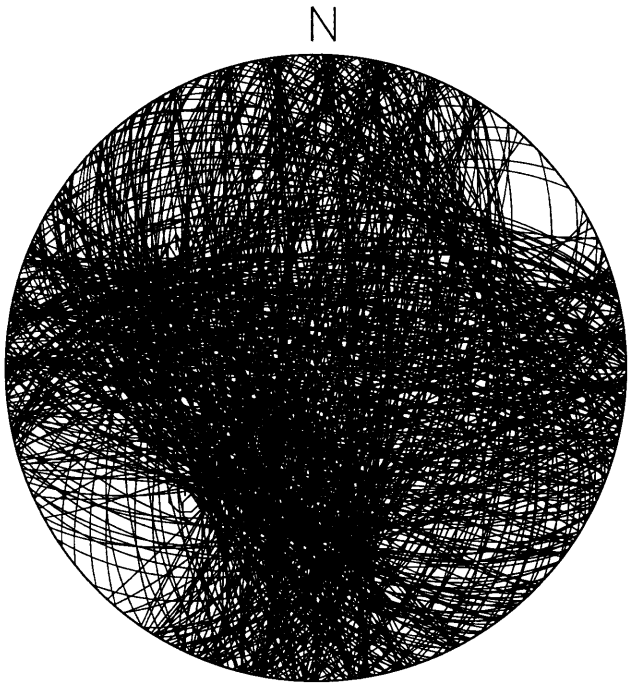

P nodal planes

Figure 10

8 MARCH 1995: ELLESMERE ISLAND, NORTHWEST TERRITORIES

Seismic Zone: none
Latitude: 82.18° N
Longitude: 71.17° W
Depth: 18 km (fixed)
Magnitude: 4.7 (mb)
Origin Time: 14:07:05 (UT)
Comments: just outside Sverdrup seismic zone

Polarity Data

Station	Distance (km)	Azimuth (°)	Take-off Angle (°)	First Motion
ALE	136	70.2	–82.5	C
RES	976	223.1	49.1	C
MBC	1154	261.4	49.1	C
DAG	1172	89.5	49.1	C
GDH	1507	152.3	48.8	C
SPITS	1543	58.3	48.0	+
FRB	2062	174.7	47.4	C
INK	2158	261.6	45.1	D
YKW3	2501	235.3	38.7	D
ARCES	2522	63.3	35.0	C
DAWY	2693	263.7	35.5	D
FCC	2705	208.2	35.5	C
ILT	2840	303.0	34.3	D
ANM	3022	289.2	33.1	–
BALM	3024	264.9	33.1	+
SCHQ	3058	174.6	33.0	–
PMR	3098	272.0	33.0	+
FFC	3212	216.7	32.8	–

Station	Distance (km)	Azimuth (°)	Take-off Angle (°)	First Motion
FINES	3384	68.1	32.6	C
ULM	3661	208.3	32.2	D
TBO	3790	200.2	32.0	–
LMQ	3861	177.3	31.8	C
PMB	3916	239.1	31.8	–
WALA	3961	228.6	31.8	D
PNT	4002	235.0	31.5	–
SVE	4281	40.0	28.0	–
VRI	5055	74.0	26.3	C
MLR	5084	75.0	26.2	C
TUL	5205	207.0	26.0	D
MEO	5348	210.0	25.8	D
MDJ	5808	341.0	24.4	C
NJ2	7325	350.0	21.3	C
DANN	7574	23.0	20.5	D
PYUN	7597	24.0	20.5	D
GYA	7853	2.0	19.9	C

Focal Mechanism Solutions

Strike	Dip	Rake
45.60	78.18	–46.87
44.58	79.98	–45.14
46.02	78.56	–44.87
43.22	80.33	–43.14
44.70	78.96	–42.87

total number solutions: 5
grid search: 2°
misfits: 3
comments: DAG, GDH, ANM, BALM and PMR polarities provided by the pIDC; ILT, SVE, VRI, MLR, TUL, MEO, MDJ, NJ2, DANN, PYUN and GYA from the ISC

misfits at MDJ, NJ2 and GYA for all solutions (note that authors did not see seismograms for any of these stations)

using only data seen by authors, we get the same solutions but with no misfits

Preferred solution:

Plane 1:
- Strike: 80°
- Dip: 45°
- Rake: –45°

Plane 2:
- Strike: 145°
- Dip: 46°
- Rake: –166°

P-axis:
- Trend: 354°
- Plunge: 38°

T-axis:
- Trend: 102°
- Plunge: 22°

B-axis:
- Trend: 215°
- Plunge: 44°

Quality: A

good azimuthal coverage; good redundancy; large number of observations

Figure Captions:

Figure 11a-e. Seismograms from which polarity data were read by the authors.

Figure 12. Focal mechanism solutions. Lower hemisphere projection. The P and T axes are shown on the left and the P nodal planes on the right. Data are also plotted. Solid symbols indicate compressional first motions and open symbols dilatations.

ELLESMERE ISLAND, NORTHWEST TERRITORIES: 8 MARCH 1995

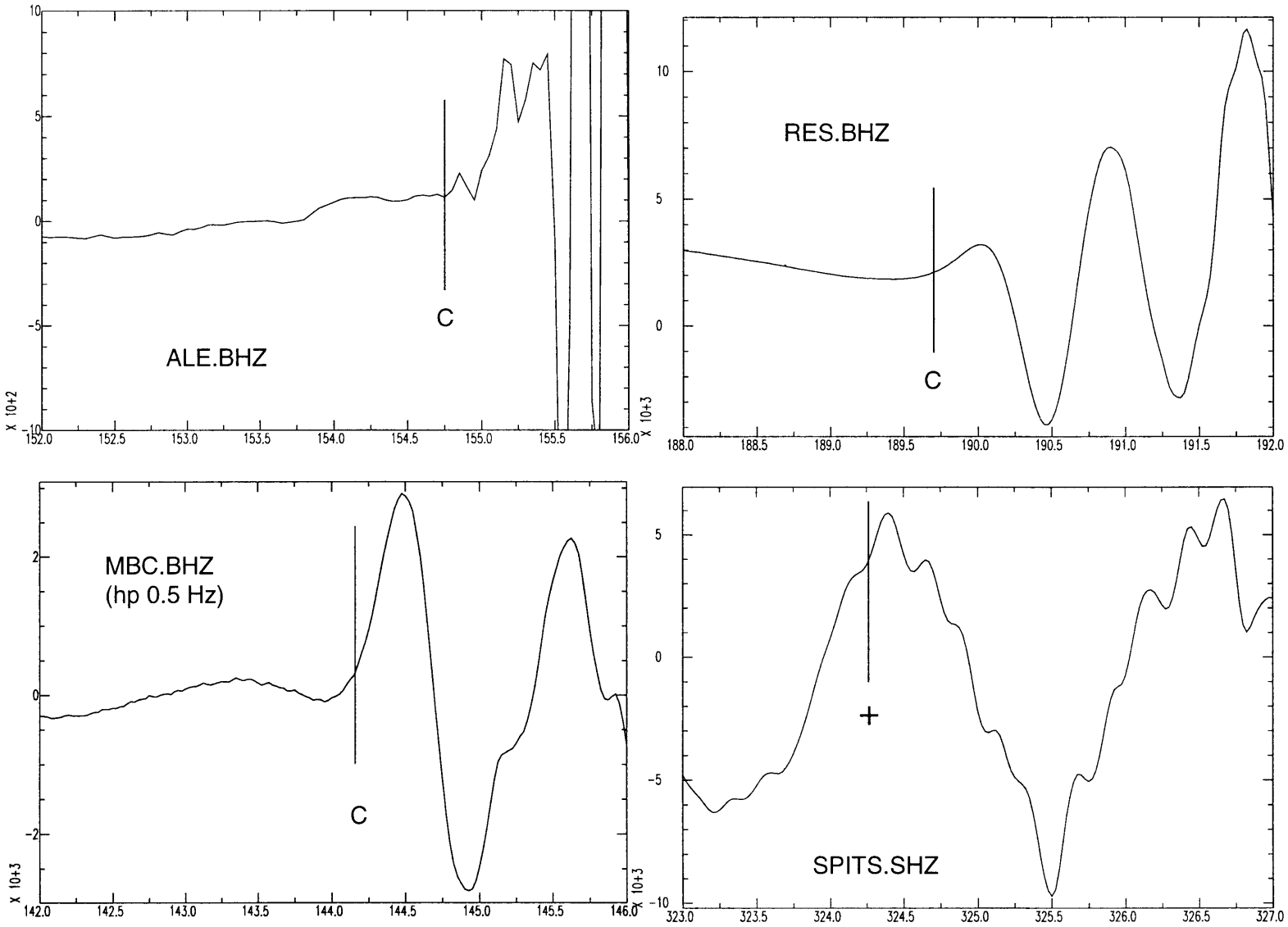

Figure 11a

ELLESMERE ISLAND, NORTHWEST TERRITORIES: 8 MARCH 1995

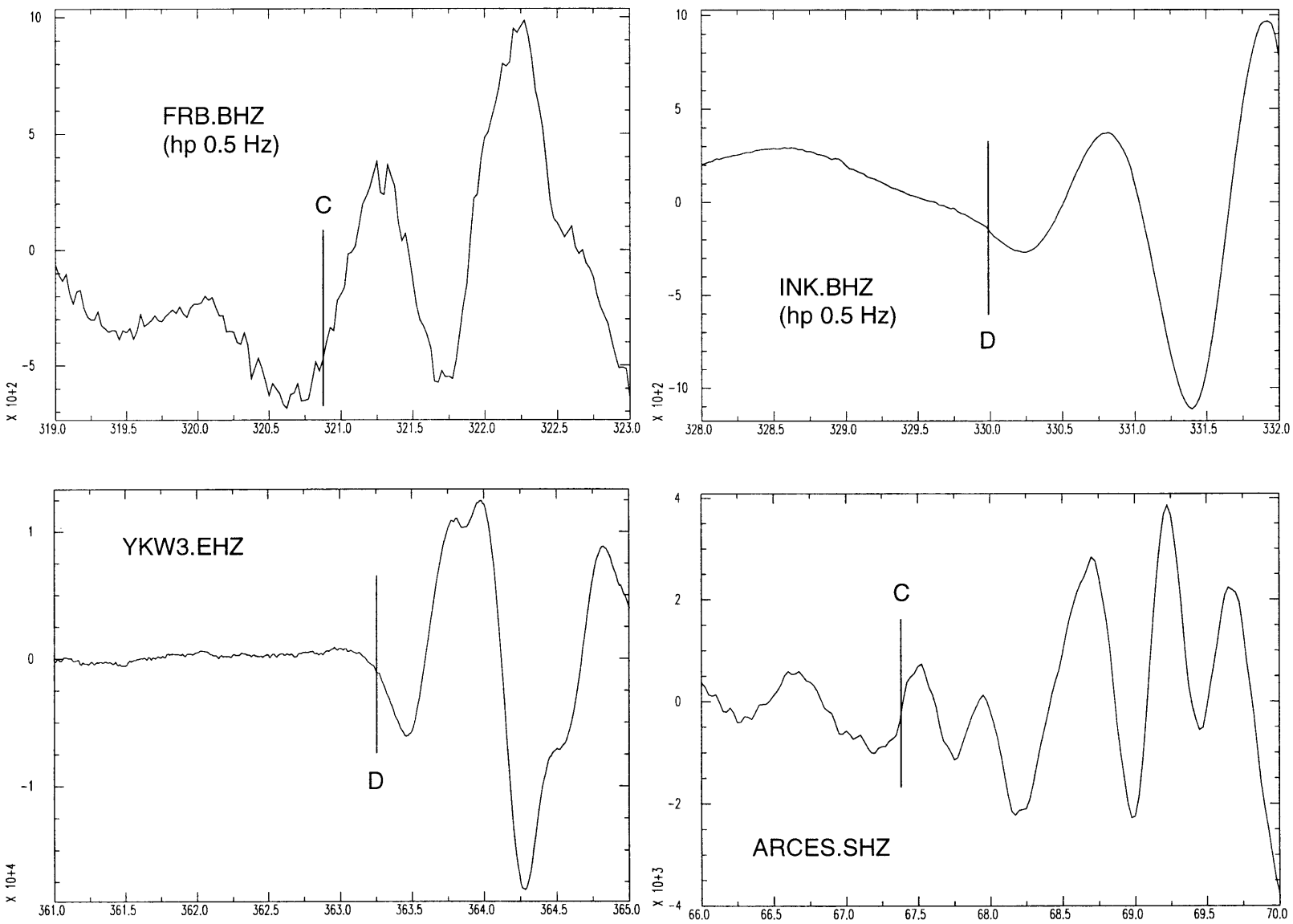

Figure 11b

ELLESMERE ISLAND, NORTHWEST TERRITORIES: 8 MARCH 1995

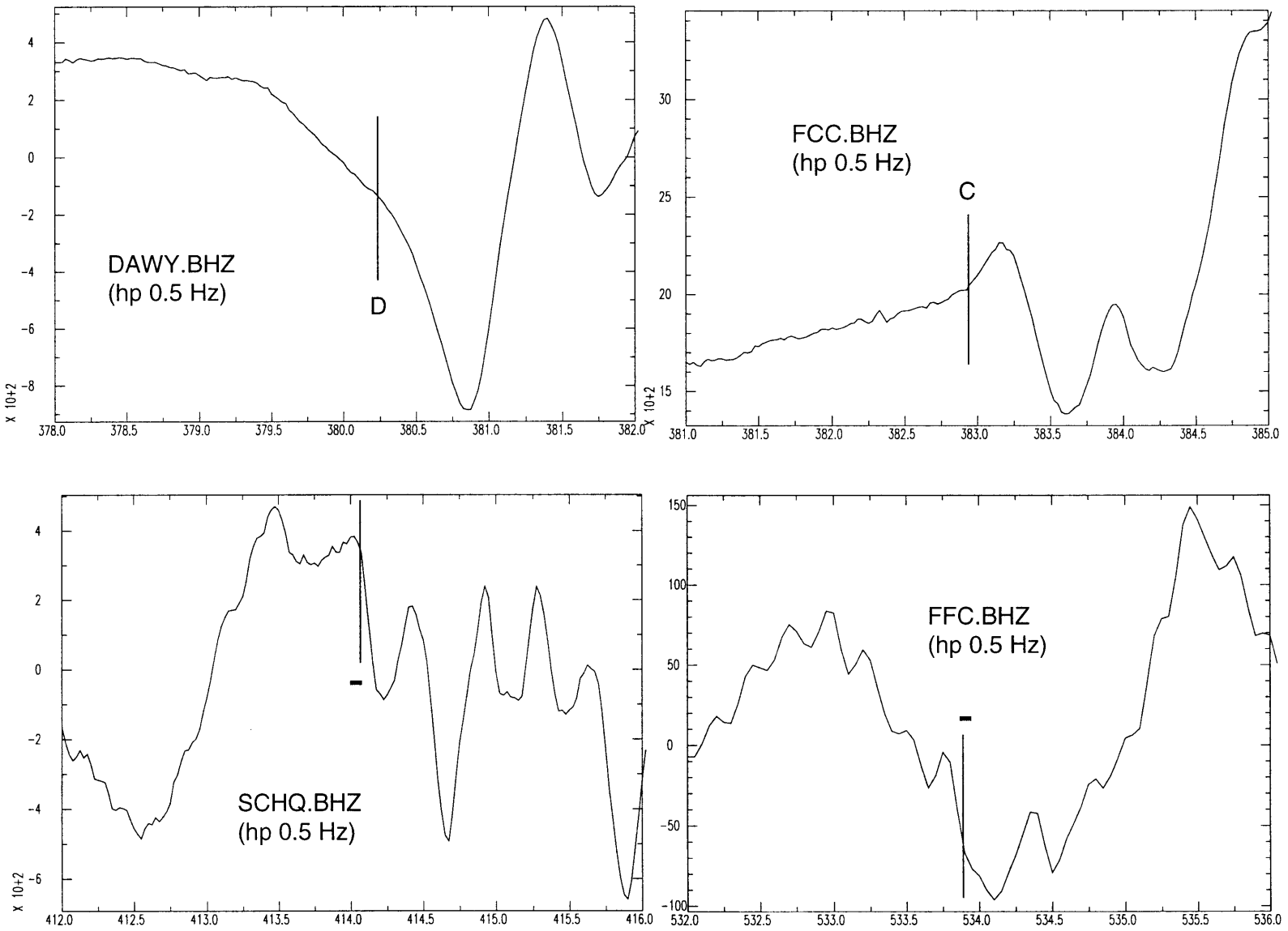

Figure 11c

ELLESMERE ISLAND, NORTHWEST TERRITORIES: 8 MARCH 1995

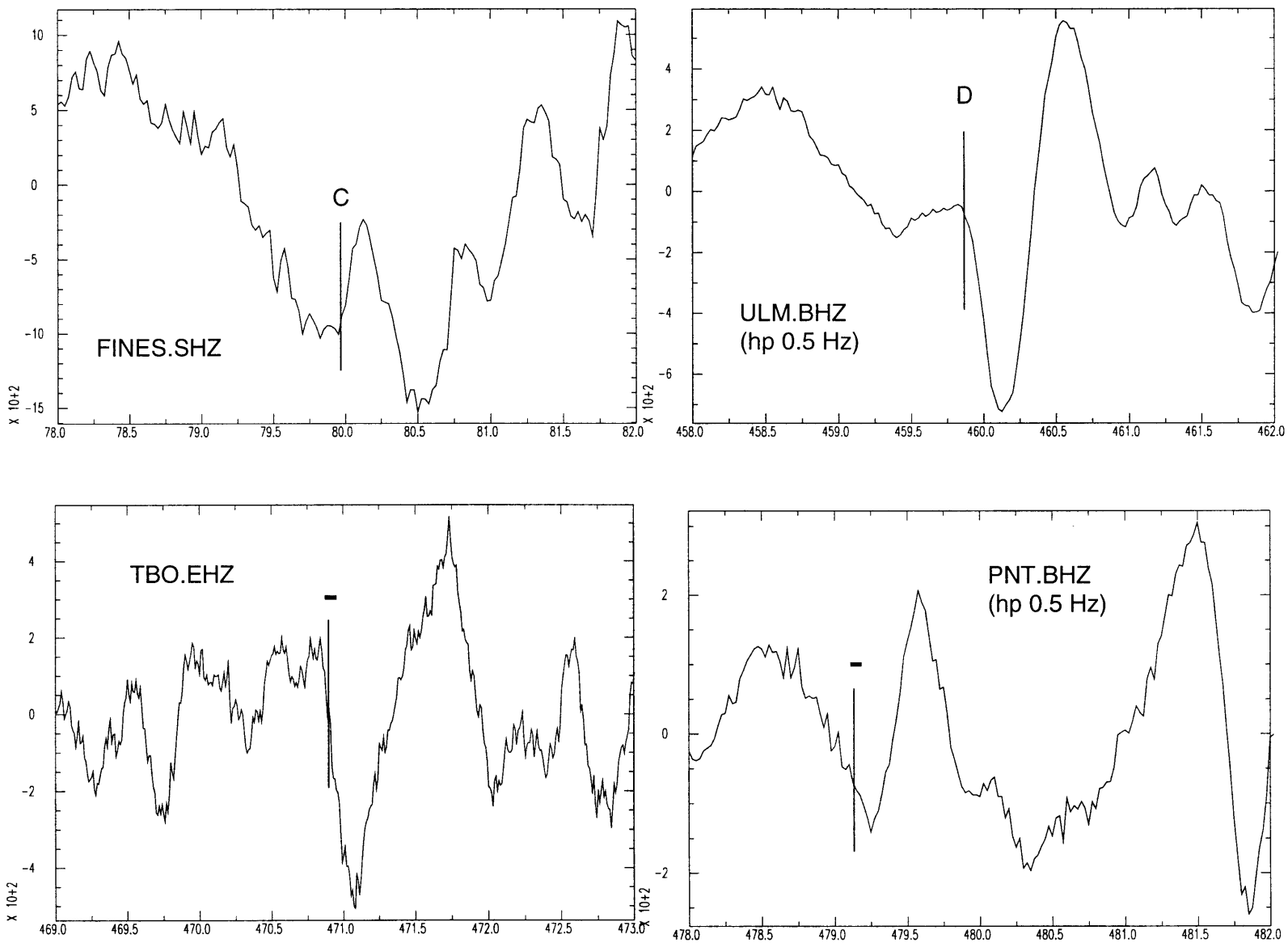

Figure 11d

ELLESMERE ISLAND, NORTHWEST TERRITORIES: 8 MARCH 1995

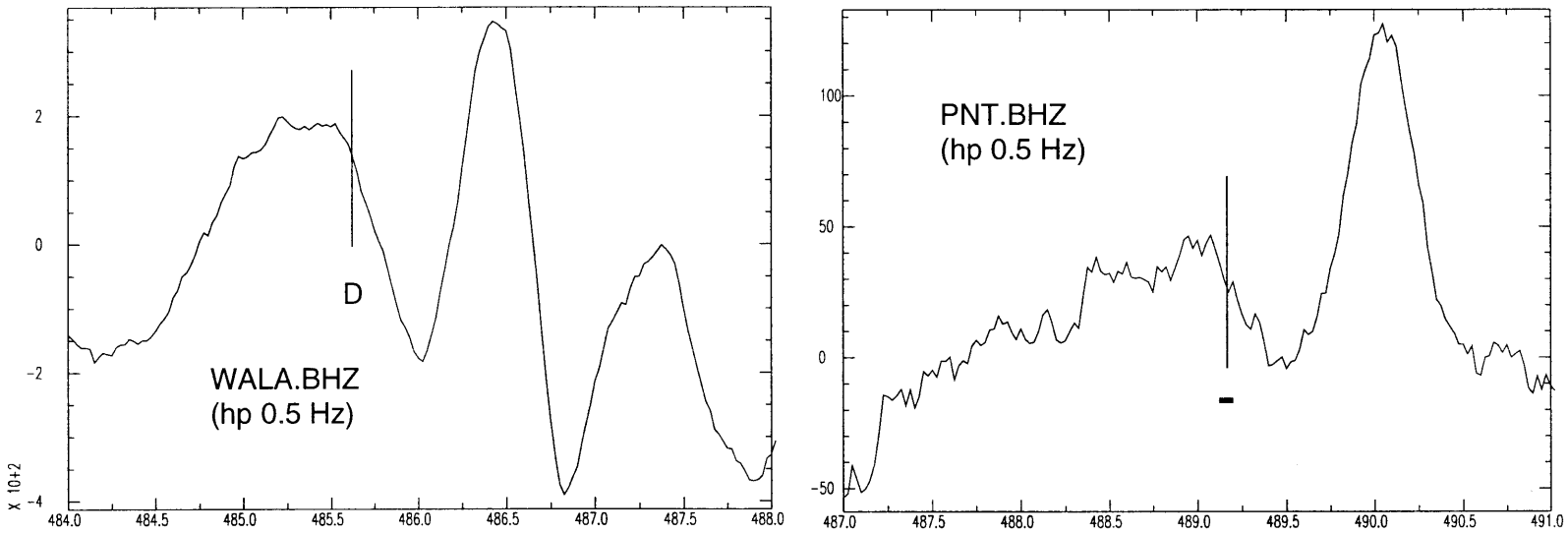

Figure 11e

ELLESMERE ISLAND, NORTHWEST TERRITORIES: 8 MARCH 1995

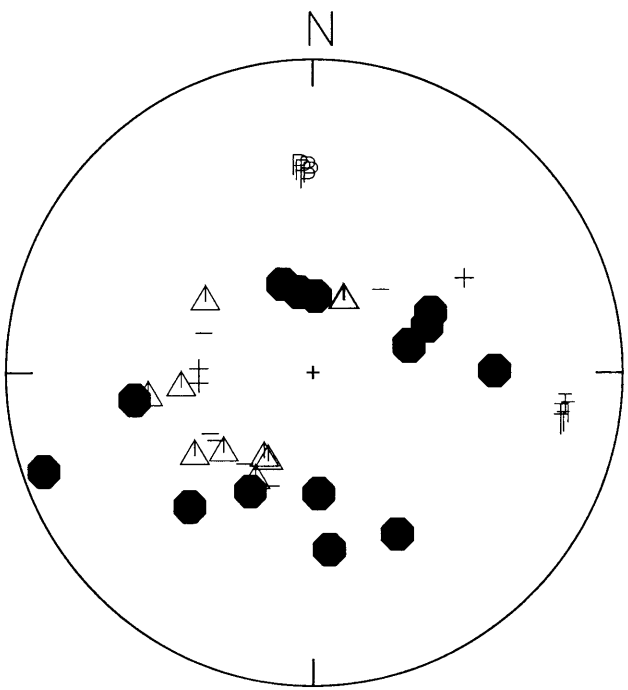

P and T axes

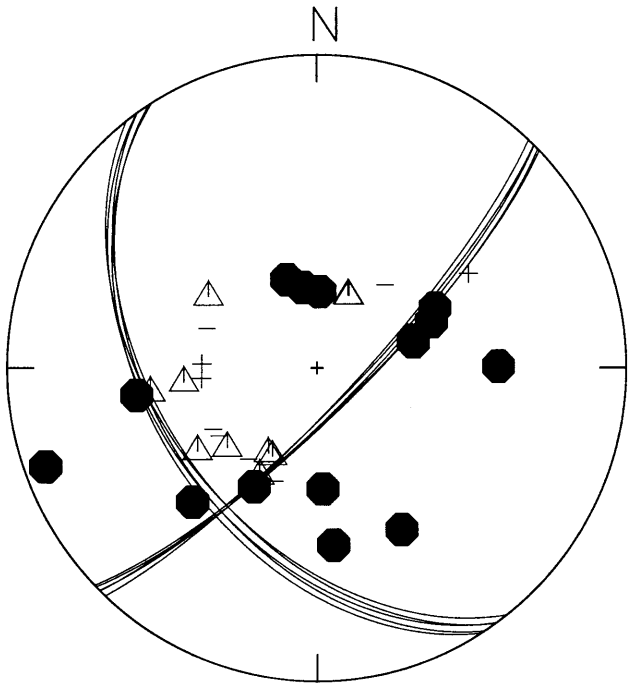

P nodal planes

Figure 12

10 MARCH 1995: ELLESMERE ISLAND, NORTHWEST TERRITORIES

Seismic Zone:	none
Latitude:	82.22° N
Longitude:	71.10° W
Depth:	18 km (fixed)
Magnitude:	4.0 (mN)
Origin Time:	00:36:58 (UT)
Comments:	just outside Sverdrup seismic zone; possible aftershock of 8 March 1995 earthquake

Polarity Data

Station	Distance (km)	Azimuth (°)	Take-off Angle (°)	First Motion
ALE	134	80.3	–82.3	D
RES	980	222.3	49.1	C
MBC	1156	260.0	49.1	C
GDH	1513	149.8	49.1	C
INK	2159	261.0	40.7	D
YKW3	2504	235.0	34.7	D
FCC	2710	208.0	32.1	C

Focal Mechanism Solutions

Strike	Dip	Rake
113.41	58.68	–60.35
114.18	58.23	–47.57
86.41	63.94	–44.31
89.09	67.48	–45.90
92.96	63.94	–44.31
97.07	60.50	–42.39

Strike	Dip	Rake
99.50	63.94	–44.31
103.61	60.50	–42.39
109.38	60.00	–35.26

total number solutions: 9
grid search: 5°
misfits: 0
comments: GDH polarity provided by the pIDC

Preferred solution:

Plane 1:
- Strike: 100°
- Dip: 64°
- Rake: –44°

Plane 2:
- Strike: 213°
- Dip: 51°
- Rake: –146°

P-axis:
- Trend: 60°
- Plunge: 49°

T-axis:
- Trend: 159°
- Plunge: 8°

B-axis:
- Trend: 255°
- Plunge: 40°

Quality: C

poor azimuthal coverage (although not unreasonable given epicentral location and earthquake magnitude)

Figure Captions:

Figure 13a-b. Seismograms from which polarity data were read by the authors.

Figure 14. Focal mechanism solutions. Lower hemisphere projection. The P and T axes are shown on the left and the P nodal planes on the right. Data are also plotted. Solid symbols indicate compressional first motions and open symbols dilatations.

ELLESMERE ISLAND, NORTHWEST TERRITORIES: 10 MARCH 1995

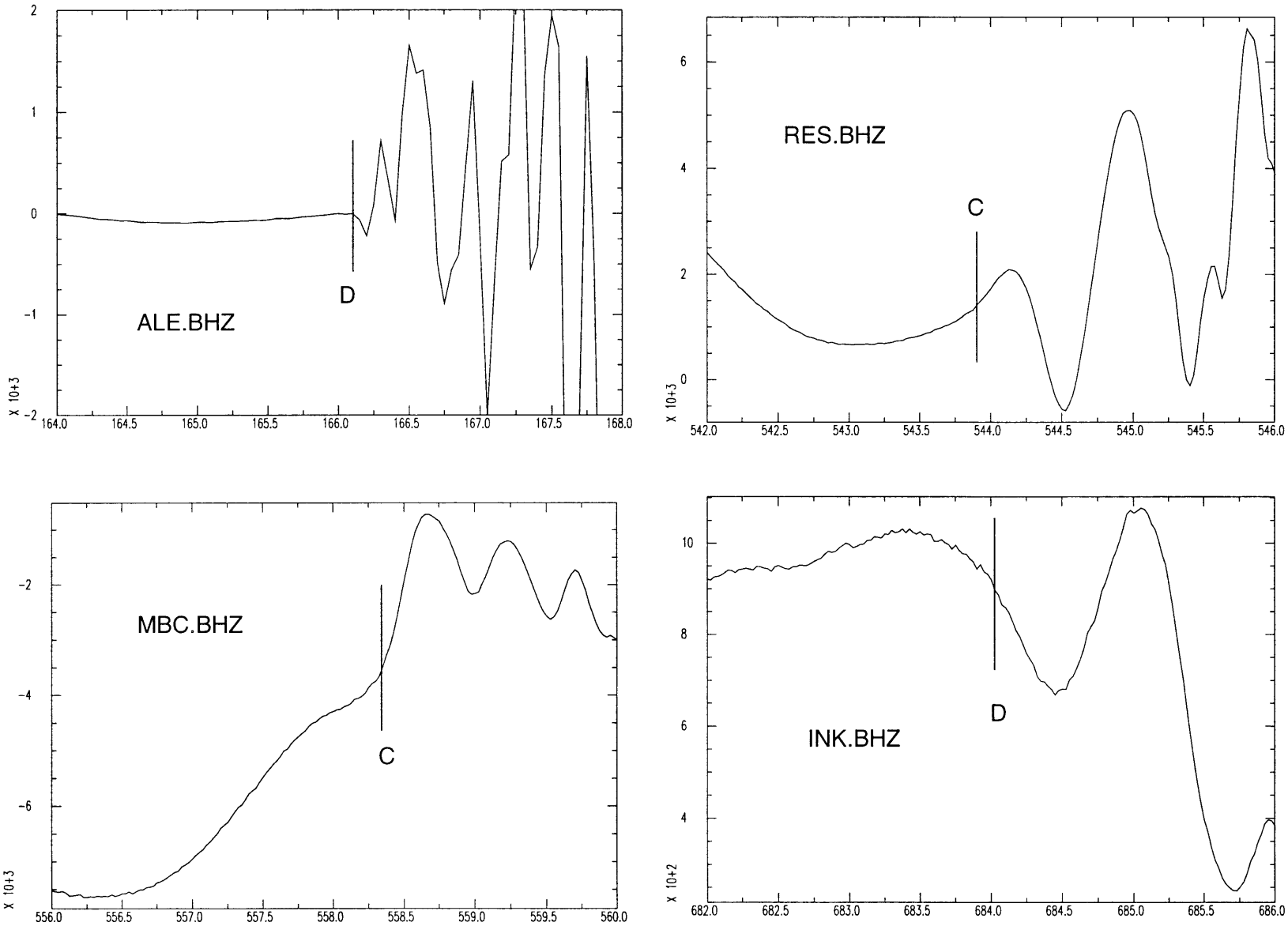

Figure 13a

ELLESMERE ISLAND, NORTHWEST TERRITORIES: 10 MARCH 1995

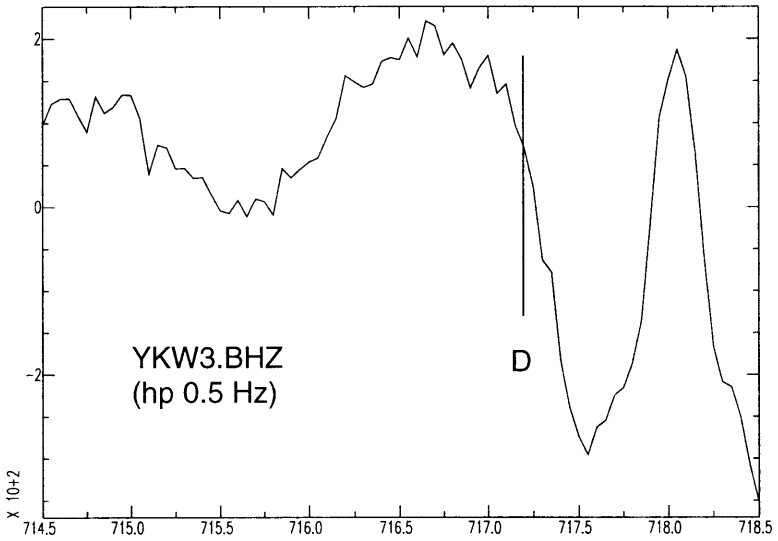

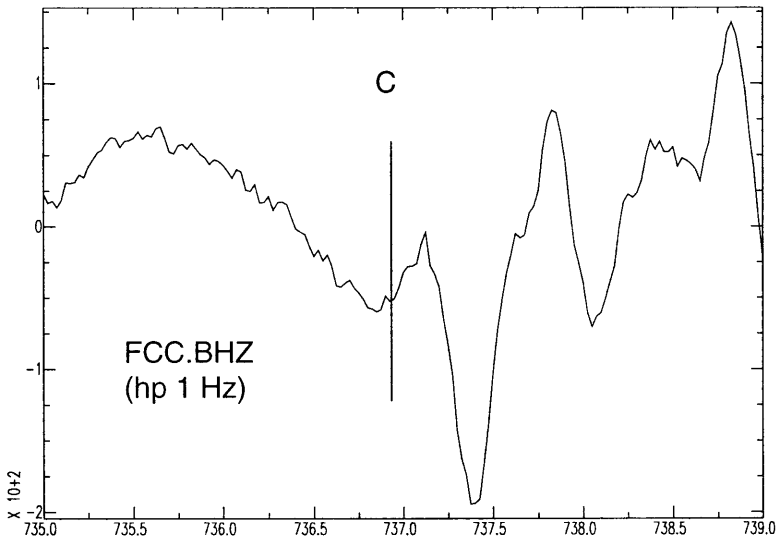

Figure 13b

ELLESMERE ISLAND, NORTHWEST TERRITORIES: 10 MARCH 1995

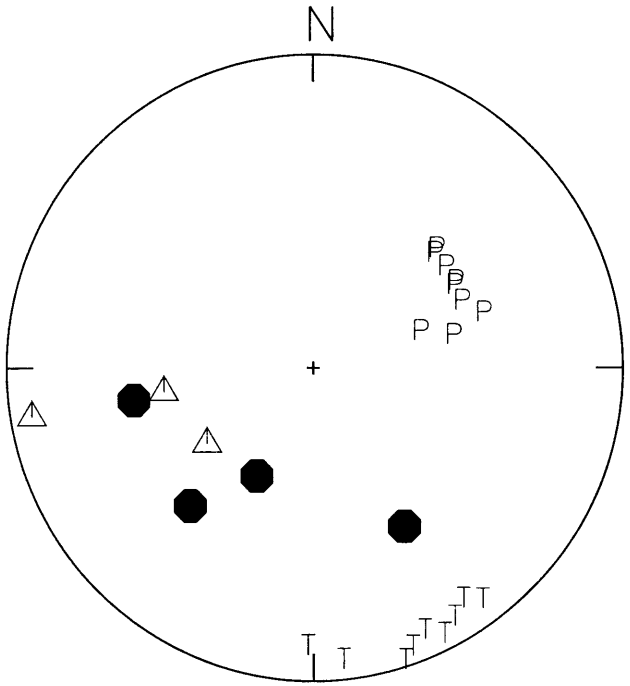

P and T axes

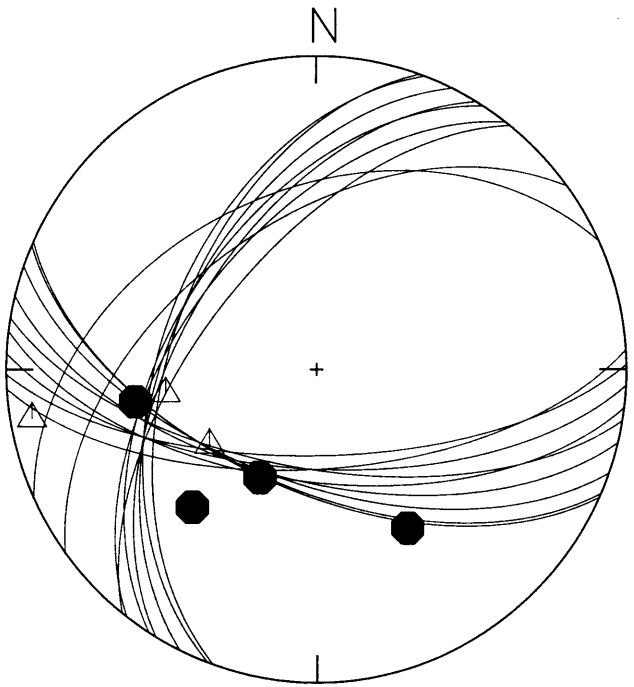

P nodal planes

Figure 14

19 MARCH 1995: BAFFIN ISLAND, NORTHWEST TERRITORIES

Seismic Zone: Baffin Island
Latitude: 66.66° N
Longitude: 62.36° W
Depth: 18 km (fixed)
Magnitude: 4.6 (mN)
Origin Time: 18:59:30 (UT)
Comments:

Polarity Data

Station	Distance (km)	Azimuth (°)	Take-off Angle (°)	First Motion
FRB	435	225	49.1	D
GDH	470	47.9	49.1	C
IGL	864	299	49.1	C
SCHQ	1341	193	49.1	D
RES	1471	321	49.1	–
FCC	1821	256.4	51.6	C
A64	2145	196	45.1	–
EEO	2437	212	38.7	D
GAC	2462	205	38.7	-
CRLO	2464	209	38.7	D
YKW3	2469	284	38.7	C

Focal Mechanism Solutions

total number solutions: 136
grid search: 5°
misfits: 0
comments: solutions from weighted data (see Methods section); Insufficient data for constrained solution

Preferred solution:

Nodal Planes:		
	Strike:	most solutions have 1 plane in the S to SW octant and the other striking NW-SE; a few solutions have both planes near east-west
	Dip:	NW-SE planes have steep dip; all others moderate
	Rake:	strike-slip (with small normal or thrust component) or oblique thrust
Plane 2:		
	Strike:	303°
	Dip:	69°
	Rake:	-139°
P-axis:		
	Trend:	near north-south
	Plunge:	shallow to moderate
T-axis:		
	Trend:	near east-west
	Plunge:	shallow
B-axis:		
	Trend:	W to NW octant
	Plunge:	steep for most solutions but could be also some shallow

Figure Captions:

Figure 15a-c. Digital seismograms from which polarity data were read by the authors.

Figure 16. Focal mechanism solutions. Lower hemisphere projection. The P and T axes are shown on the left and the P nodal planes on the right. Data are also plotted. Solid symbols indicate compressional first motions and open symbols dilatations.

19 MARCH 1995: BAFFIN ISLAND, NORTHWEST TERRITORIES

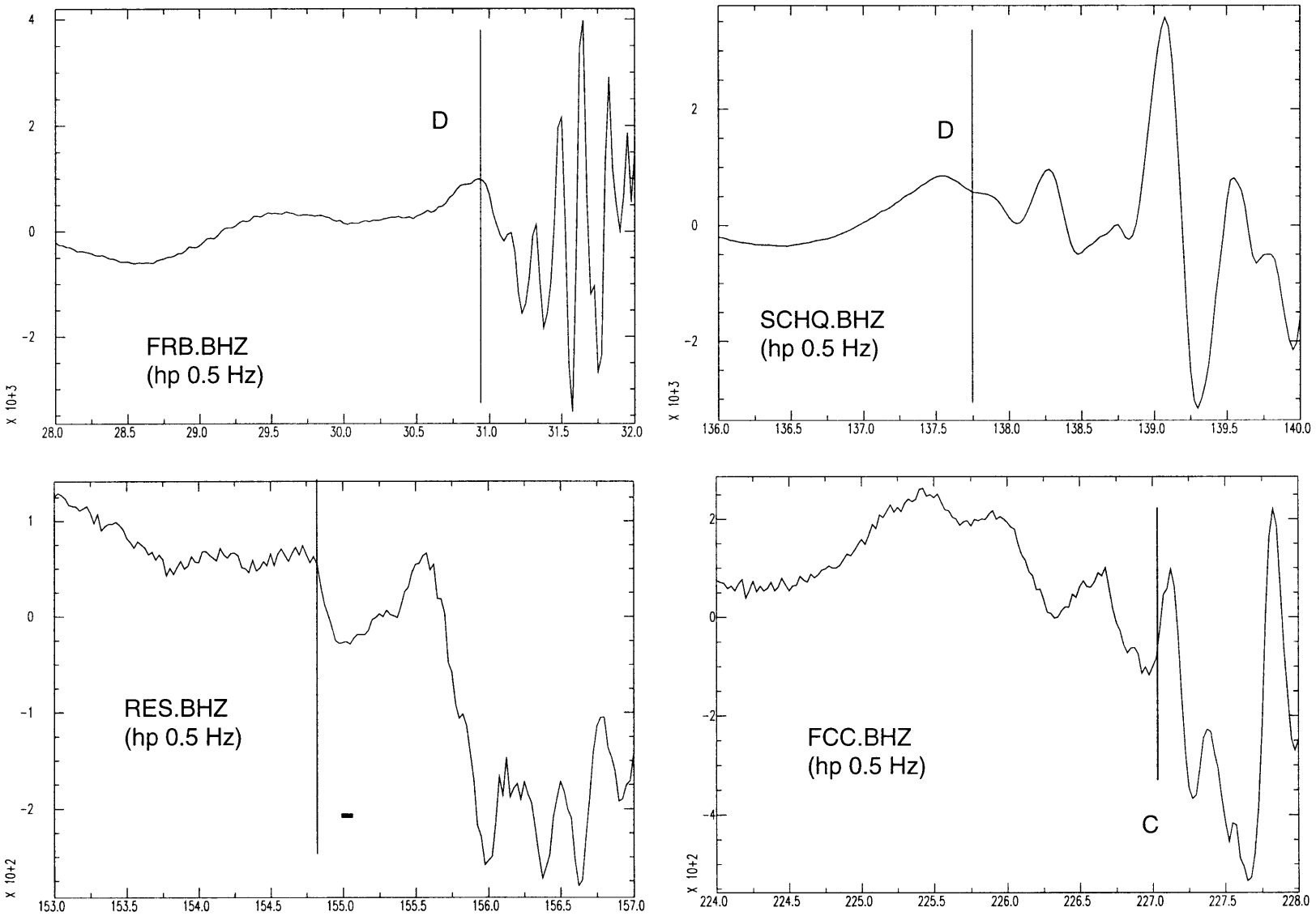

Figure 15a

19 MARCH 1995: BAFFIN ISLAND, NORTHWEST TERRITORIES

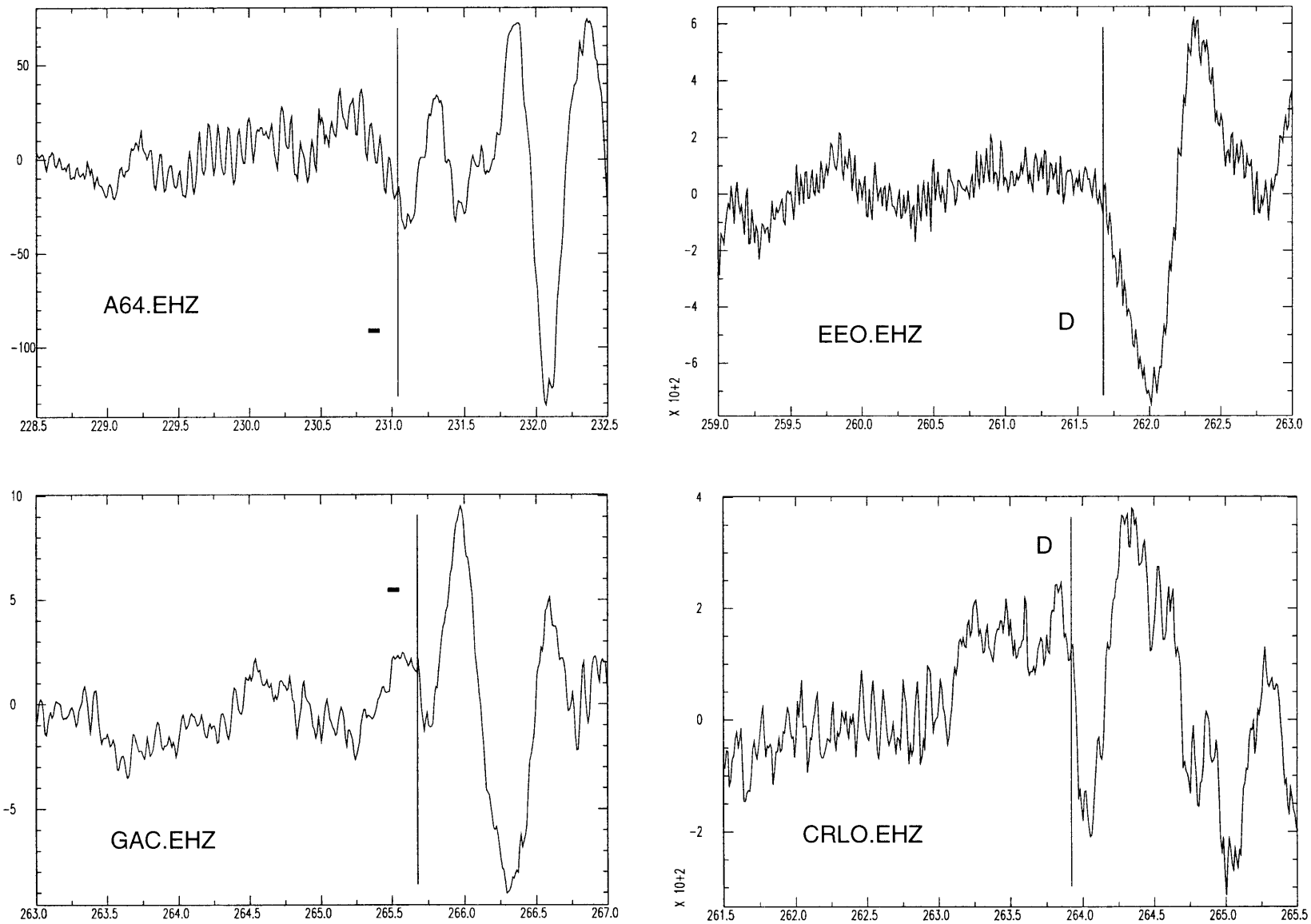

Figure 15b

19 MARCH 1995: BAFFIN ISLAND, NORTHWEST TERRITORIES

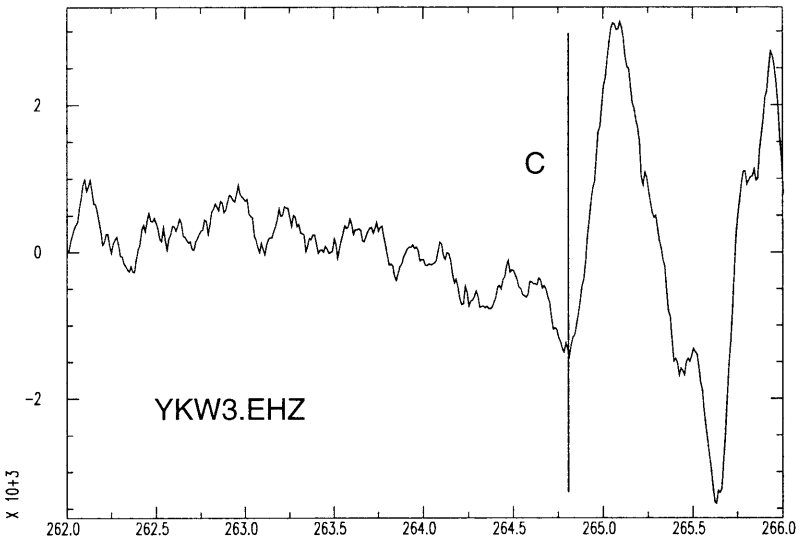

Figure 15c

BAFFIN ISLAND, NORTHWEST TERRITORIES: 19 MARCH 1995

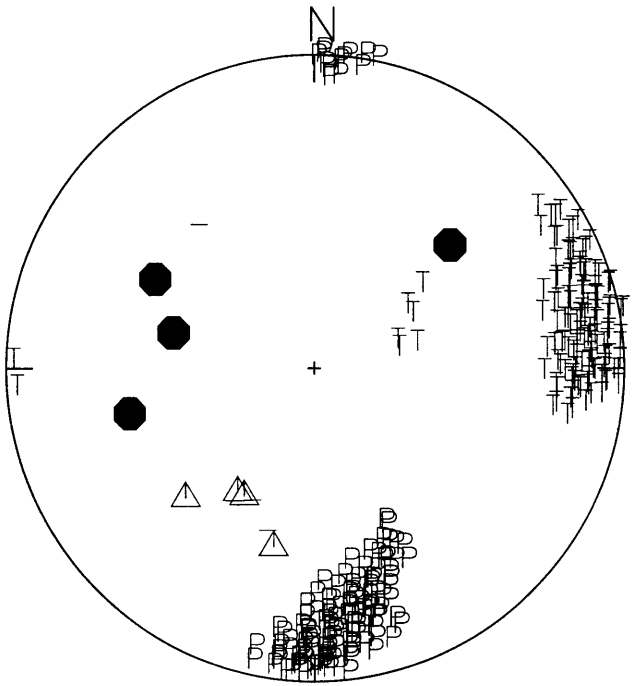

P and T axes

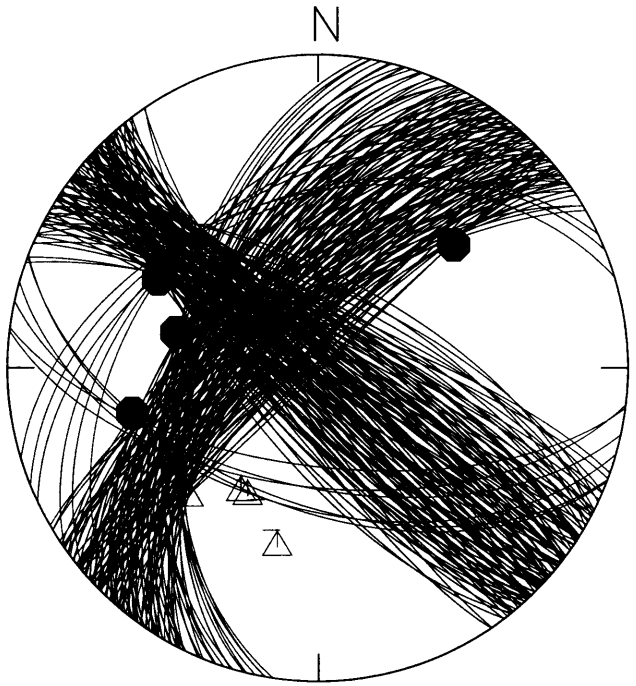

P nodal planes

Figure 16

18 JULY 1995: LABRADOR SEA

Seismic Zone: Labrador Sea
Latitude: 61.00° N
Longitude: 59.55° W
Depth: 18 km (fixed)
Magnitude: 4.2 (ML)
Origin Time: 05:37:23 (UT)
Comments:

Polarity Data

Station	Distance (km)	Azimuth (°)	Take-off Angle (°)	First Motion
FRB	557	307.3	49.1	C
SCHQ	812	215.3	49.1	-
JAQ	1256	237.5	49.1	D
SMQ	1282	203.6	49.1	–
MNQ	1300	210.3	49.1	-
DRLN	1316	173.5	49.1	C
ICQ	1369	204.3	49.1	+
IGL	1387	321.6	49.1	D
CNQ	1410	206.2	49.1	+
A21	1618	208.3	49.1	D
A61	1630	209.2	49.1	C
TRQ	1913	217.4	49.6	D
GRQ	1920	220.7	49.6	-
FCC	1930	277.9	49.6	C
GAC	1996	218.6	47.4	C

Focal Mechanism Solutions

Strike	Dip	Rake
74.21	80.42	-39.03

total number solutions: 1
grid search: 5°
misfits: 1
comments: misfits A21; same solutions results if weighting scheme used and emergent data included; fits all emergent stations except MNQ

Preferred solution:

Plane 1:
- Strike: 74°
- Dip: 80°
- Rake: -39°

Plane 2:
- Strike: 172°
- Dip: 52°
- Rake: -168°

P-axis:
- Trend: 26°
- Plunge: 34°

T-axis:
- Trend: 129°
- Plunge: 19°

B-axis:
- Trend: 243°
- Plunge: 50°

Quality: C
moderate azimuthal coverage; some redundancy

Figure Captions:

Figure 17a-d. Seismograms from which polarity data were read by the authors.

Figure 18. Focal mechanism solutions. Lower hemisphere projection. The P and T axes are shown on the left and the P nodal planes on the right. Data are also plotted. Solid symbols indicate compressional first motions and open symbols dilatations.

18 JULY 1995: LABRADOR SEA

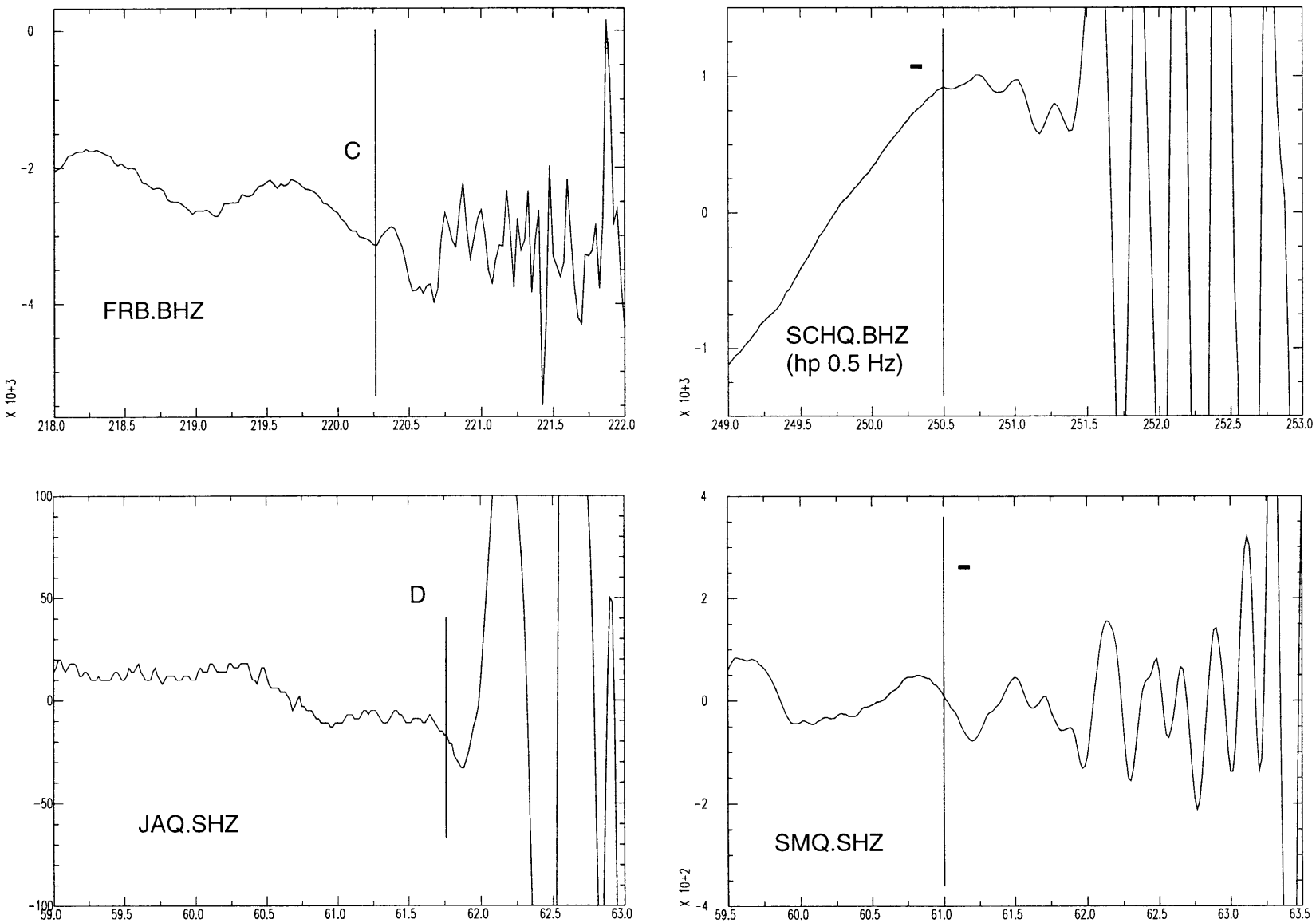

Figure 17a

18 JULY 1995: LABRADOR SEA

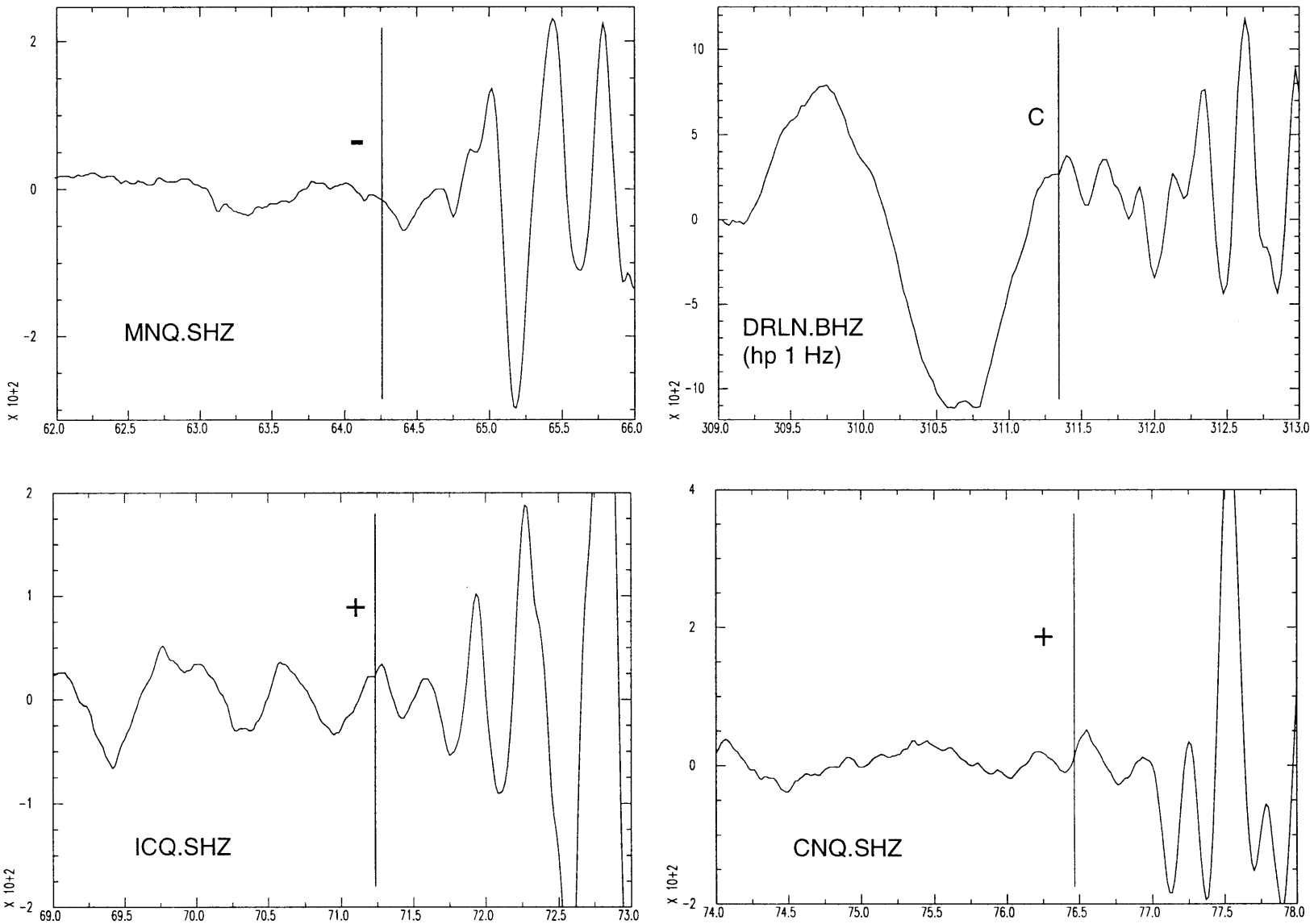

Figure 17b

18 JULY 1995: LABRADOR SEA

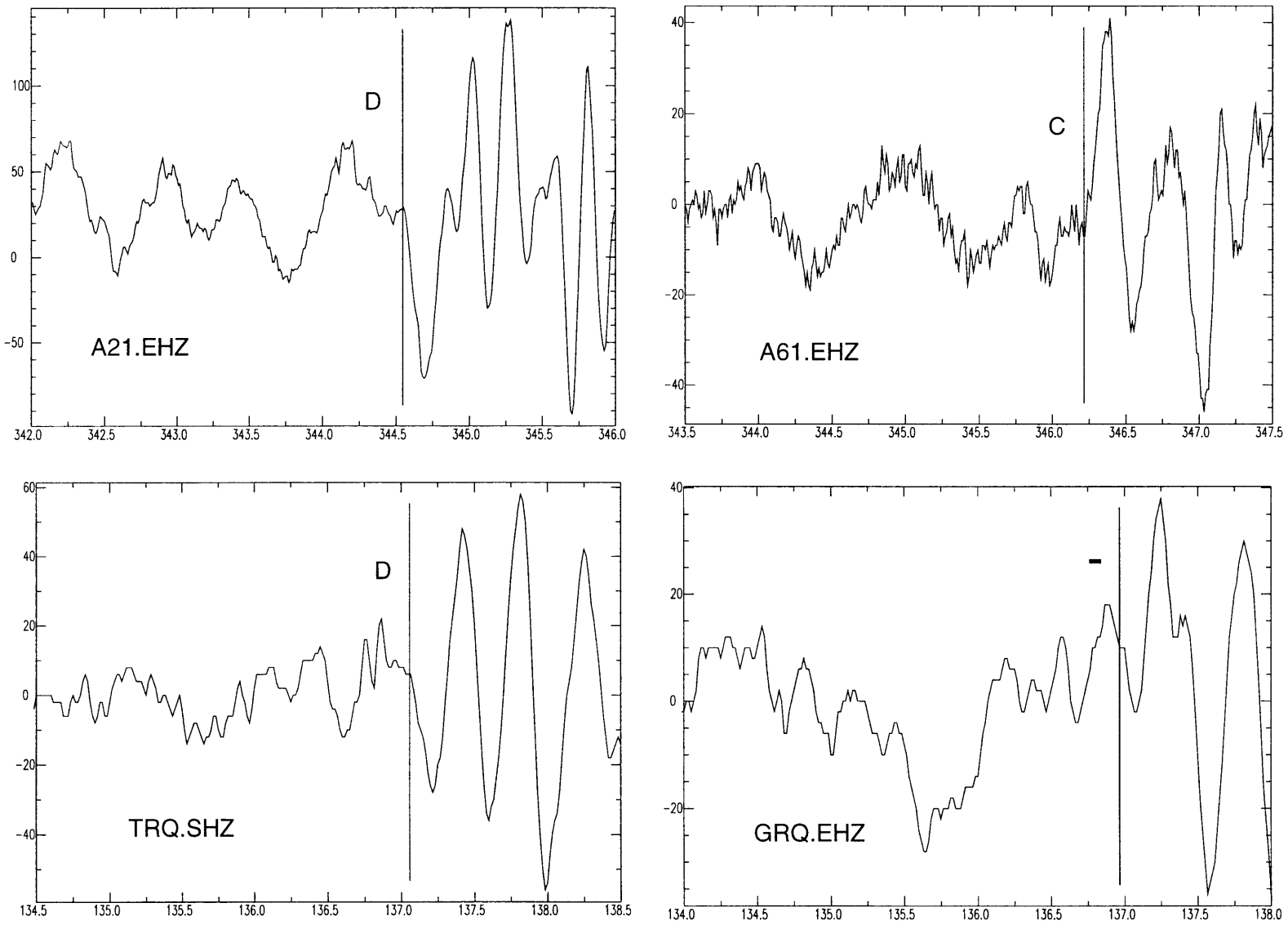

Figure 17c

18 JULY 1995: LABRADOR SEA

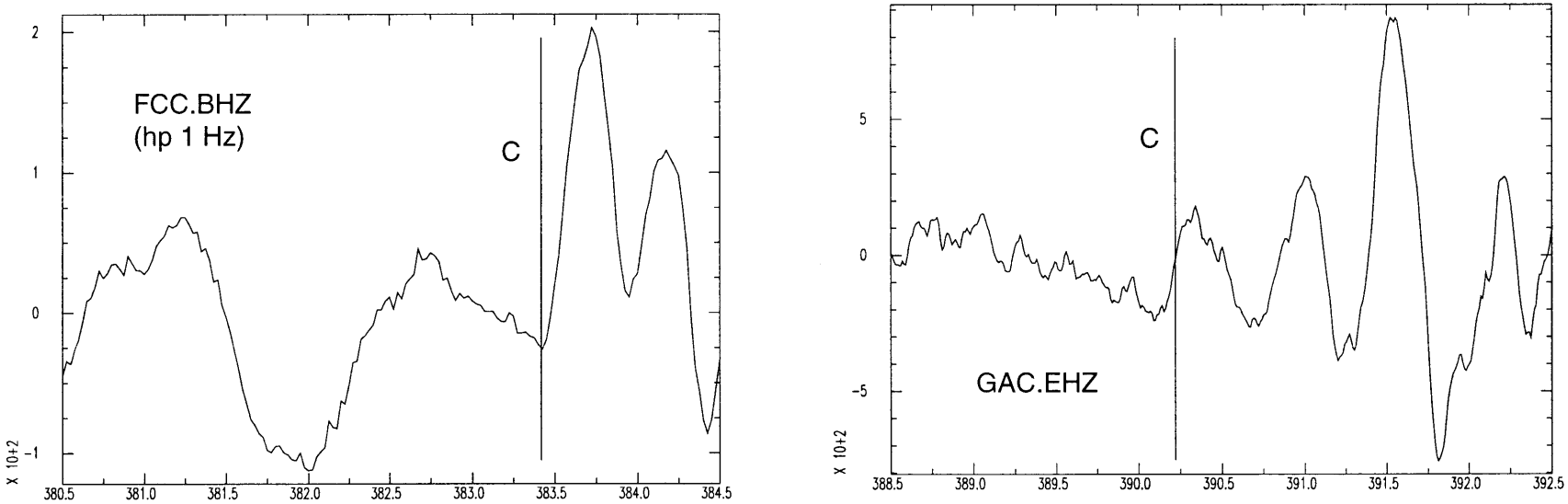

Figure 17d

Labrador Sea: July 18 1995

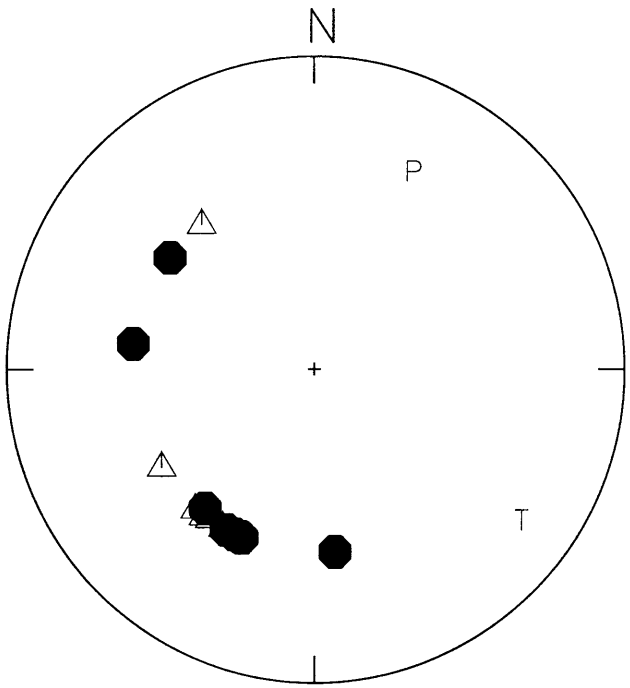

P and T axes

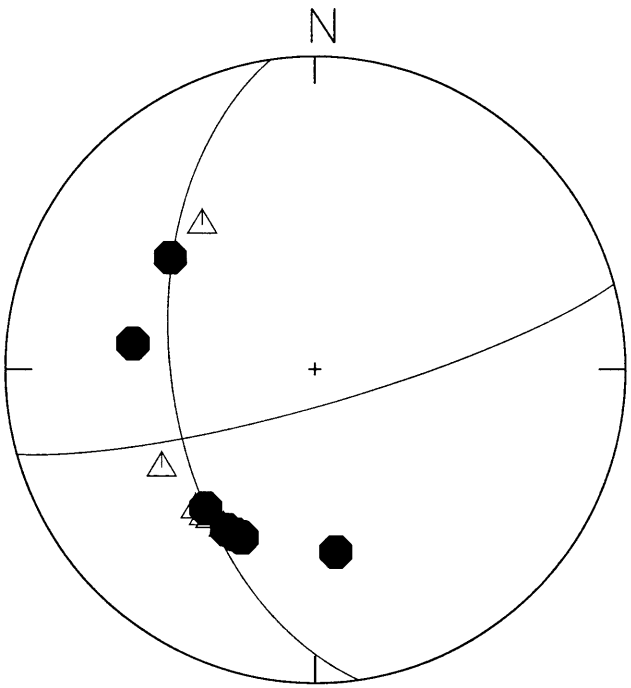

P nodal planes

Figure 18

24 AUGUST 1995: BYAM MARTIN CHANNEL, NORTHWEST TERRITORIES

Seismic Zone: Gustaf-Lougheed Arch
Latitude: 77.10° N
Longitude: 106.18° W
Depth: 18 km (fixed)
Magnitude: 4.6 (mN)
Origin Time: 12:16:49 (UT)
Comments:

Polarity Data

Station	Distance (km)	Azimuth (°)	Take-off Angle (°)	First Motion
MBC	352	260.8	49.1	C
RES	408	125.7	49.1	C
ALE	1085	33.1	49.1	+
INK	1315	236.5	49.1	C
DAWY	1857	237.0	49.6	C
FCC	2100	160.3	45.10	C
DLBC	2276	217.5	42.8	D
WHY	2120	226.4	45.1	-
HYT	2152	230.2	45.1	C

Focal Mechanism Solutions

Strike	Dip	Rake
215.41	87.13	34.90
215.91	81.46	34.07

total number solutions: 2
grid search: 5°
misfits: 0
comments: solutions based on weighted data (see Methods section)

Preferred solution:

Plane 1:
- Strike: 215°
- Dip: 87°
- Rake: 35°

Plane 2:
- Strike: 123°
- Dip: 55°
- Rake: 177°

P-axis:
- Trend: 344°
- Plunge: 22°

T-axis:
- Trend: 85°
- Plunge: 26°

B-axis:
- Trend: 220°
- Plunge: 55°

Quality: B

fairly good azimuthal coverage; some redundancy

Figure Captions:

Figure 19a-c. Seismograms from which polarity data were read by the authors.

Figure 20. Focal mechanism solutions. Lower hemisphere projection. The P and T axes are shown on the left and the P nodal planes on the right. Data are also plotted. Solid symbols indicate compressional first motions and open symbols dilatations.

24 AUGUST 1995 (1216): BYAM MARTIN CHANNEL, NORTHWEST TERRITORIES

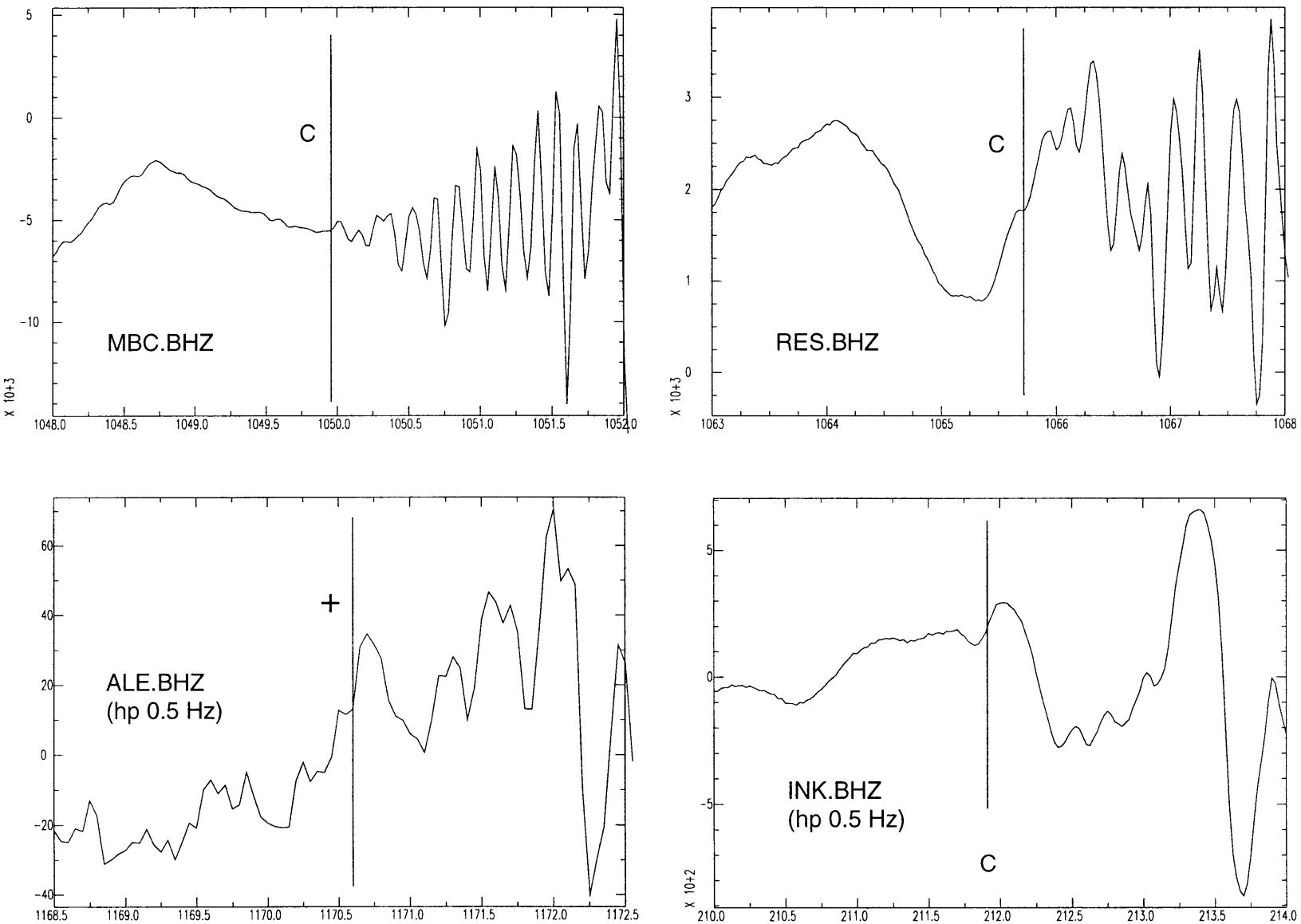

Figure 19a

BYAM MARTIN CHANNEL, NORTHWEST TERRITORIES: 24 AUGUST 1995 (1216)

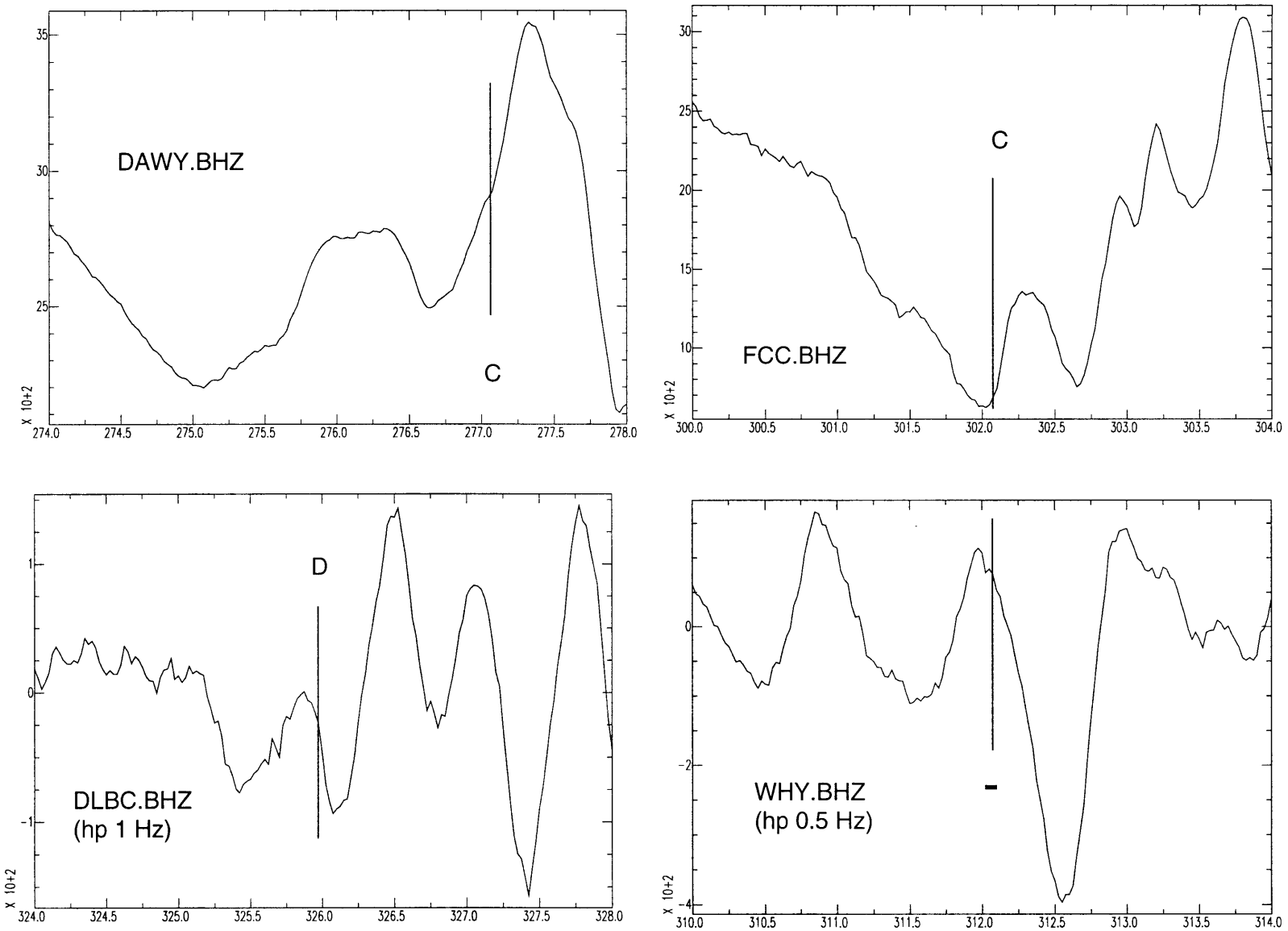

Figure 19b

24 AUGUST 1995 (1216): BYAM MARTIN CHANNEL, NORTHWEST TERRITORIES

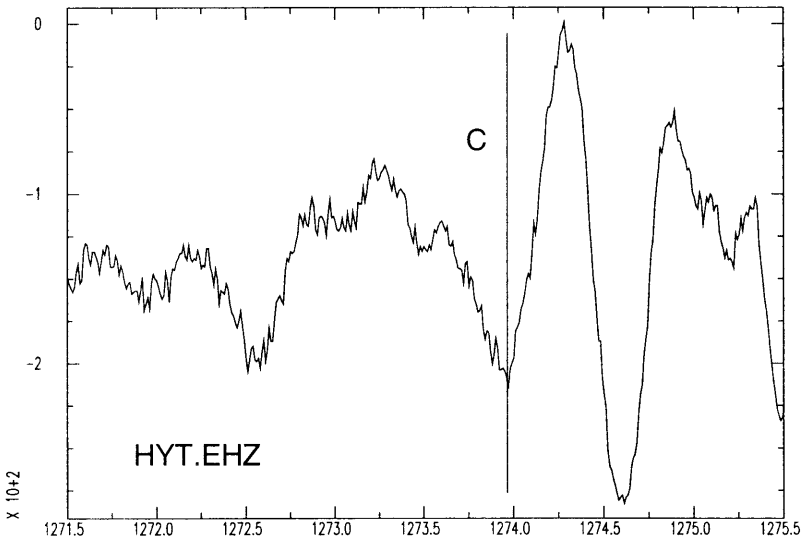

Figure 19c

Byam Martin Channel, Northwest Territories: 24 August 1995

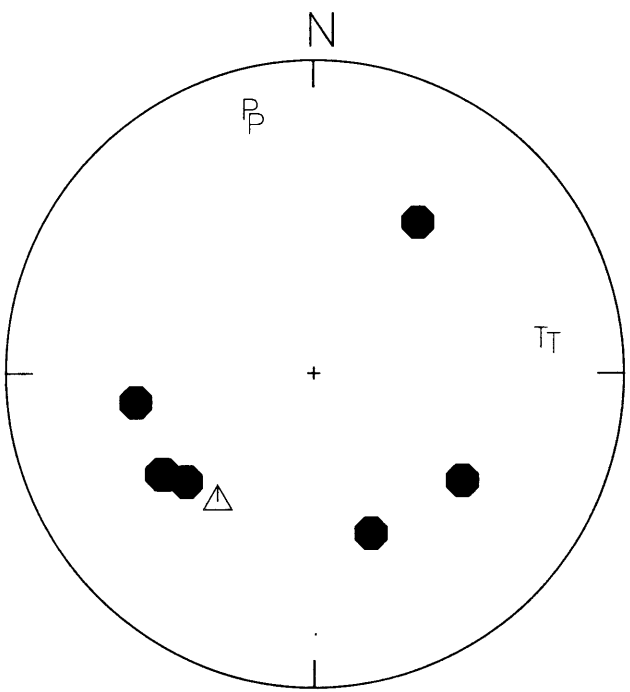

P and T axes

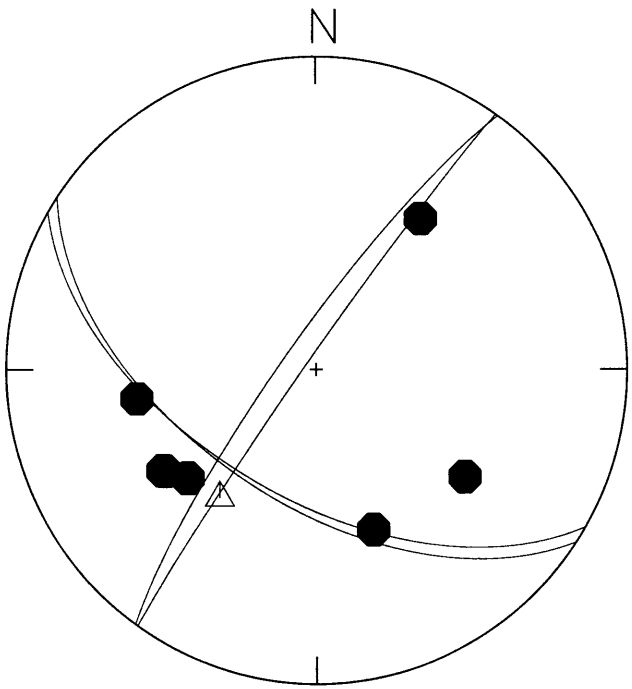

P nodal planes

Figure 20

24 AUGUST 1995: BYAM MARTIN CHANNEL, NORTHWEST TERRITORIES

Seismic Zone: Gustaf-Lougheed Arch
Latitude: 76.53° N
Longitude: 107.23° W
Depth: 18 km (fixed)
Magnitude: 4.4 (mN)
Origin Time: 14:51:42
Comments:

Polarity Data

Station	Distance (km)	Azimuth (°)	Take-off Angle (°)	First Motion
MBC	321	270.1	49.1	C
RES	399	114.9	49.1	–
INK	1257	237.1	49.5	D
YKW3	1585	194.0	48.4	D
YKW4	1590	194.2	48.3	D
DAWY	1800	237.1	46.4	D
FRB	1980	114.6	43.7	+
FCC	2051	158.0	42.5	-
WHY	2057	226.1	42.3	D
HYT	2091	230.0	45.1	D
DLBC	2210	216.9	39.6	+
EDM	2616	189.2	35.5	C

Focal Mechanism Solutions

total number solutions: 280
grid search: 5°
misfits: 0
comments: insufficient data to determine

Preferred solution:

Nodal Planes:Insufficient data to determine; most solutions oblique thrust to pure thrust, but some strike-slip and oblique normal solutions possible

P-axis:
- Trend: NE or SW quadrants
- Plunge: near horizontal

T-axis:
- Trend: NW-SE
- Plunge: insufficient data to determine

B-axis:
- Trend: NW-SE or in WSW-W octant
- Plunge: insufficient data to determine

Figure Captions:

Figure 21a-c. Seismograms from which polarity data were read by the authors.

Figure 22. Focal mechanism solutions. Lower hemisphere projection. The P and T axes are shown on the left and the P nodal planes on the right. Data are also plotted. Solid symbols indicate compressional first motions and open symbols dilatations.

24 AUGUST 1995 (1451): BYAM MARTIN CHANNEL, NORTHWEST TERRITORIES

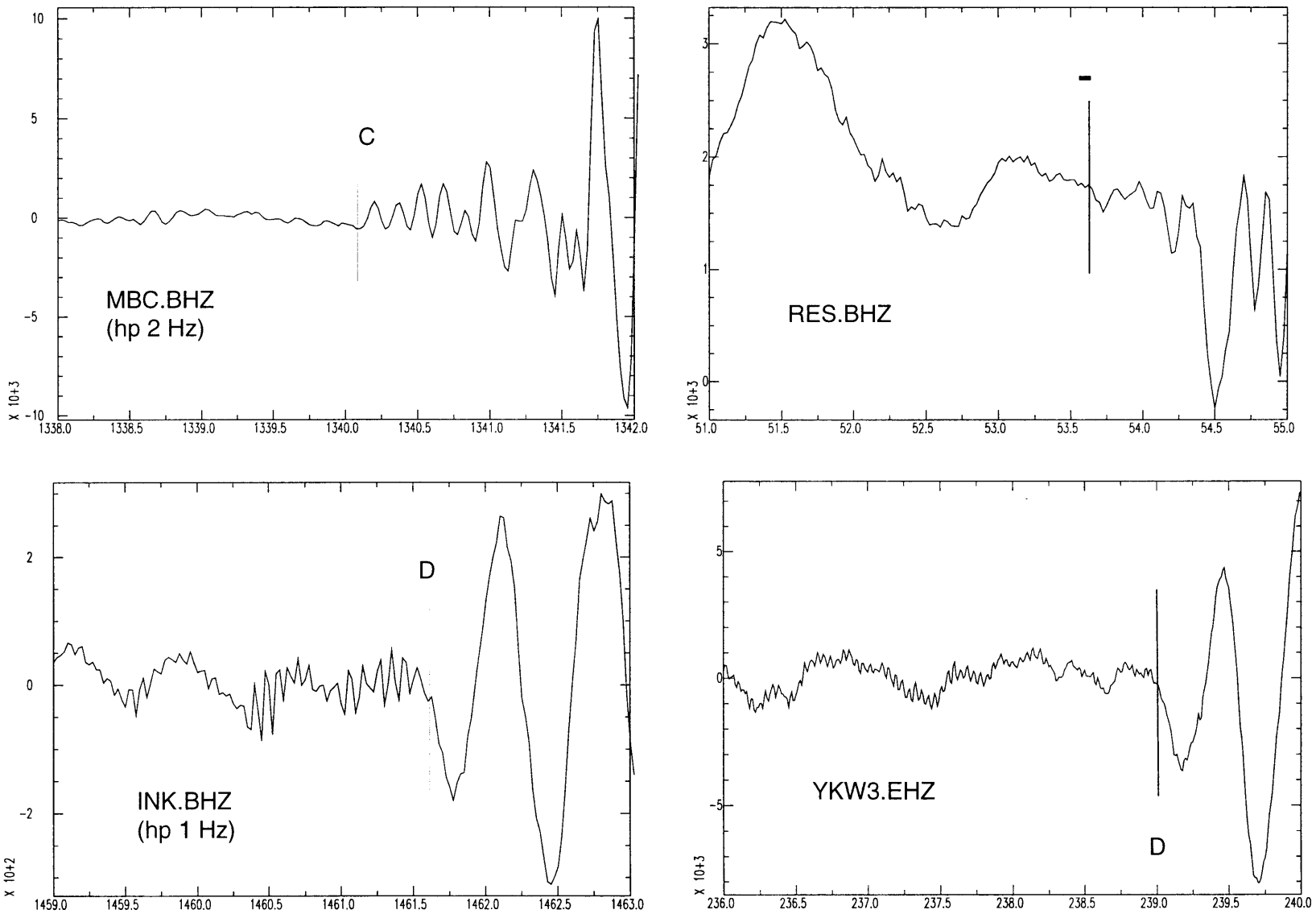

Figure 21a

24 AUGUST 1995 (1451): BYAM MARTIN CHANNEL, NORTHWEST TERRITORIES

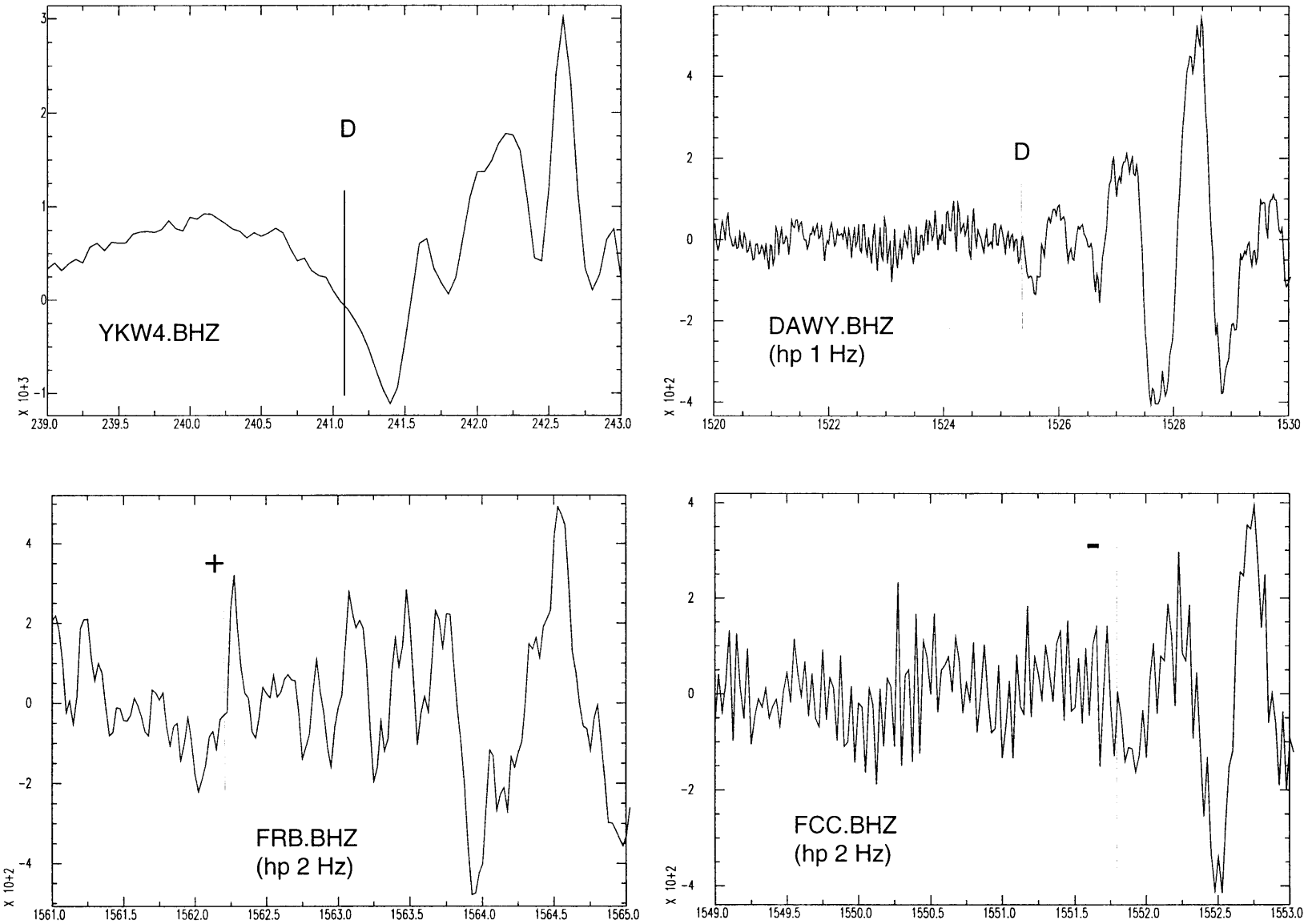

Figure 21b

24 AUGUST 1995 (1451): BYAM MARTIN CHANNEL, NORTHWEST TERRITORIES

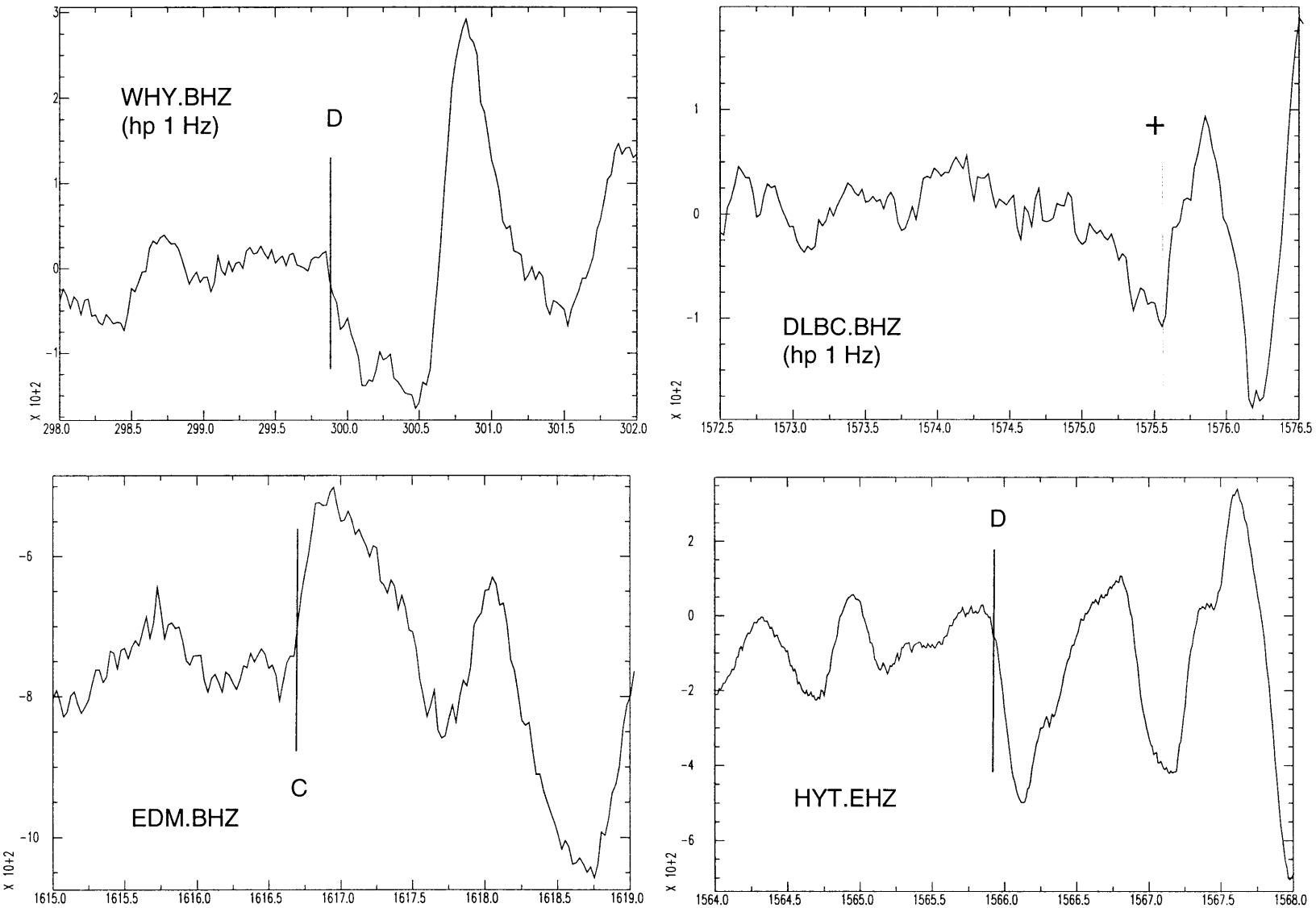

Figure 21c

BYAM MARTIN CHANNEL, NORTHWEST TERRITORIES: 24 AUGUST 1995 (1451)

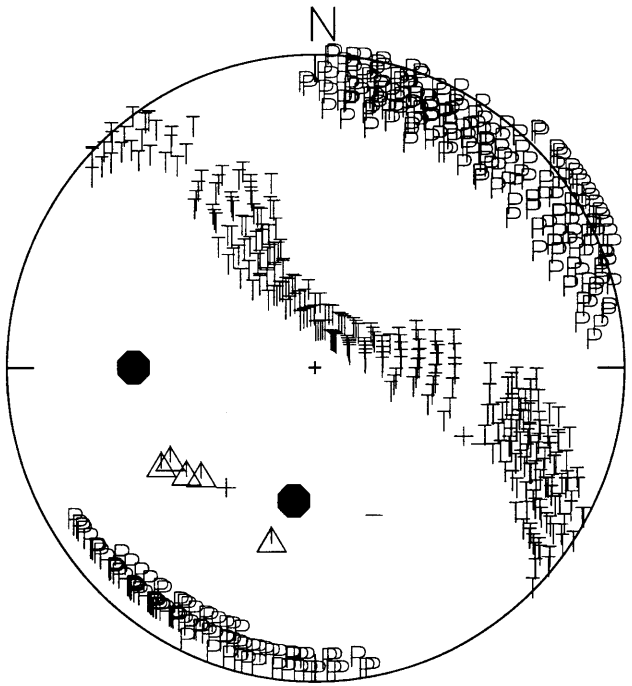

P and T axes

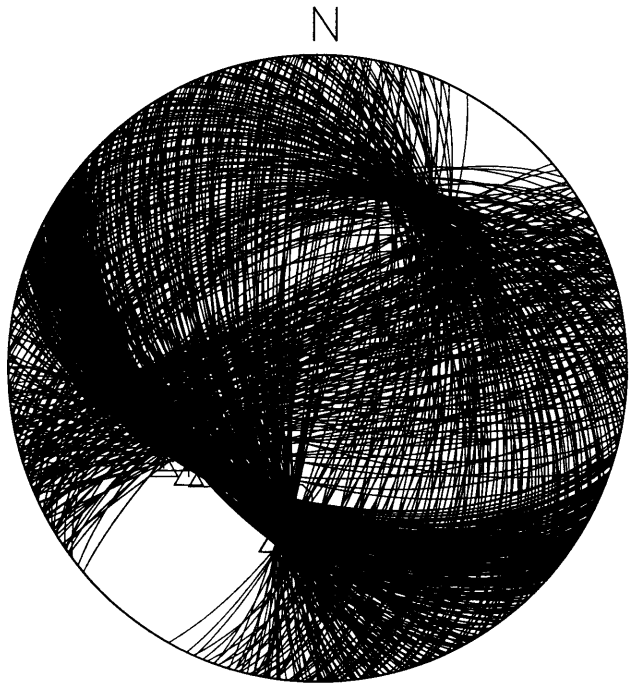

P nodal planes

Figure 22

PREVIOUSLY PUBLISHED FOCAL MECHANISMS

One of the earthquakes that fit the selection criteria for this study has been previously analyzed (Fig. 23). For completeness, we include the focal mechanism for this earthquake here, but not the data used to determine it. For more information on this earthquake, the reader should consult the original source of the focal mechanism.

25 SEPTEMBER 1994: LA MALBAIE, QUEBEC

Seismic Zone:	Charlevoix	
Latitude:	47.77° N	
Longitude:	69.96° W	
Depth:	17.2 km	
Magnitude:	4.3 (mN)	
Origin Time:	00:53:28 (UT)	
Comments:	felt in Charlevoix-Kamouraska region and as far away as northwestern New Brunswick (east), Jonquière (west), Beauport (south) and Les Escoumins (north)	
Focal Mechanism:	strike:	37°
	dip:	56°
	rake:	90°
Reference:	Lamontagne (1998)	

Figure 23: Map showing epicenter and focal mechanism for the the earthquake discussed above for which a focal mechanism solution has been previously published. Shaded regions represent compressional quadrants.

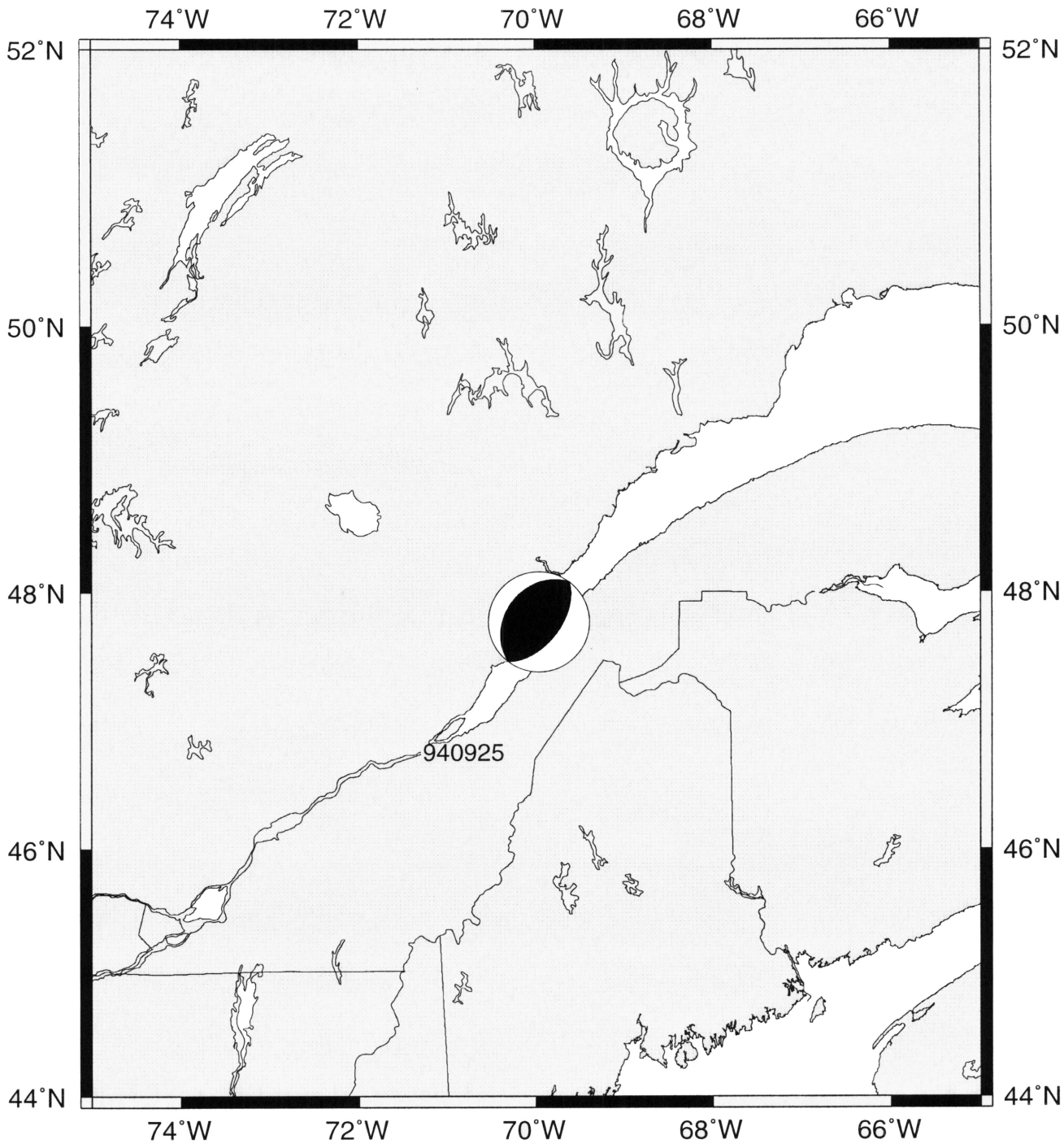

Figure 23

DISCUSSION

New Brunswick: Event 940714 has an oblique-thrust mechanism (Figure 24) on a northeast striking plane. The predominantly thrust motion is consistent with focal mechanisms of previous earthquakes in the Miramichi region (Choy *et al.*, 1983; Wetmiller *et al.*, 1984) as is the near north-south strike. However, strikes other than north-south have also been determined for other New Brunswick earthquakes (Bent and Drysdale, 2000).

Labrador Sea-Baffin Island: We were able to determine focal mechanisms for only one of the three events that occurred in this region (Figure 25). The 950718 Labrador Sea earthquake has an oblique-normal or strike-slip mechanism depending on which nodal plane is the fault plane. The mechanism is very similar to those determined for two recent events: 980521 (Bent and Perry, 1999) and 990729 (Bent and Drysdale, 2001). It is difficult to say whether these are typical focal mechanisms for the Labrador Sea as all types of faulting have been observed for earthquakes in this region (Bent and Hasegawa, 1992). Event 950319 on southern Baffin Island is either a strike-slip or oblique thrust event. We could not obtain a well-constrained solution for this event, but the solutions tended to have one NW-SE and one SSW nodal plane or two near east-west nodal plane, and moderate to steep dips. The P axis has a shallow to moderate plunge in a near north-south direction; the T axis plunges shallowly in a near east-west direction; the B axis plunges steeply and trends in the west to northwest octant. For event 950220 we can conclude only that the P-axis trends in the NW-SE direction and that the T-axis trends NE-SW. Baffin Bay and Baffin Island have consistently been the most difficult regions for which to determine focal mechanisms due to low station density and poor azimuthal coverage of stations in this region. Focal mechanisms could not be determined fot any of the wight magnitude 4.0 or greater that occurred in this region since 1994 (Bent and Perry, 1999; Bent and Drysdale 2000, 2001).

Ellesmere Island: While the mechanisms for the two Ellesmere Island events differ slightly (Figure 26), both are indicative of oblique-normal faulting. Only two other focal mechanisms are known to exist for Ellesmere Island earthquakes. The mechanism for an event on 14 April 1998 (Bent and Perry, 1999) is almost identical to that of 950308. An event on 9 June 1998 (Bent and Perry, 1999) has a strike-slip mechanism but overlaps considerably in terms of compressional and dilatational quadrants with event 980310. All four mechanisms have one similar nodal plane striking northwest-southeast and with a moderate dip to the southwest, suggesting that this is the more probable fault plane. The oblique-normal mechanisms of most of the events suggests that tectonic processes affecting Ellesmere Island may be similar to those on Baffin Island.

Byam Martin Channel: A focal mechanism was determined for event 950824a, but not for 950824b (Figure 27). The high strike-slip component for 950824a is consistent with previous studies of Byam Martin Channel earthquakes (Bent and Perry, 1999; Hasegawa, 1977). Although a focal mechanism could not be determined for event 950824b, we can constrain the P axis to be shallowly plunging in the NE-SW direction. The T axis trends NW-SE but the plunge cannot be determined. A pure normal focal mechanism can be

ruled out. An oblique-thrust solution similar to that of 950824a is consistent with the data but oblique-normal and pure thrust events will also satisfy the first motion data.

Boothia-Ungava: We were unable to determine a focal mechanism (Figure 28) for the lone earthquake in this region (940905) but can place some constraints on its stress axes. The P axis is either shallowly plunging in a NW-SE direction or is in the northeast quadrant with a moderate to steep plunge. The T axis is either in the SW quadrant or trends near-NE. The B axis is constrained only not to be in the SW quadrant. The northeast trending P axis would be more consistent with the regional trend (Adams, 1995), but deviation from this trend has been observed for some earthquakes (for example, Bent and Perry, 1999).

Figure 24. Preferred focal mechanisms for earthquakes in New Brunswick. In this and subsequent figures, focal mechanism solutions are lower hemisphere projections with shaded regions represented compressional quadrants. Symbol size is scaled to magnitude. Earthquakes are identified by date. A and B quality solutions have black shading; C and D quality solutions are shaded in gray and a "?" indicates that a solution could not be obtained.

Figure 25. Preferred focal mechanisms for earthquakes in the Labrador Sea to Baffin Bay-Baffin Island region.

Figure 26. Preferred focal mechanisms for earthquakes on Ellesmere Island.

Figure 27. Preferred focal mechanisms for earthquakes in the Byam Martin Channel.

Figure 28. Preferred focal mechanisms for earthquakes in the Boothia-Ungava seismic zone.

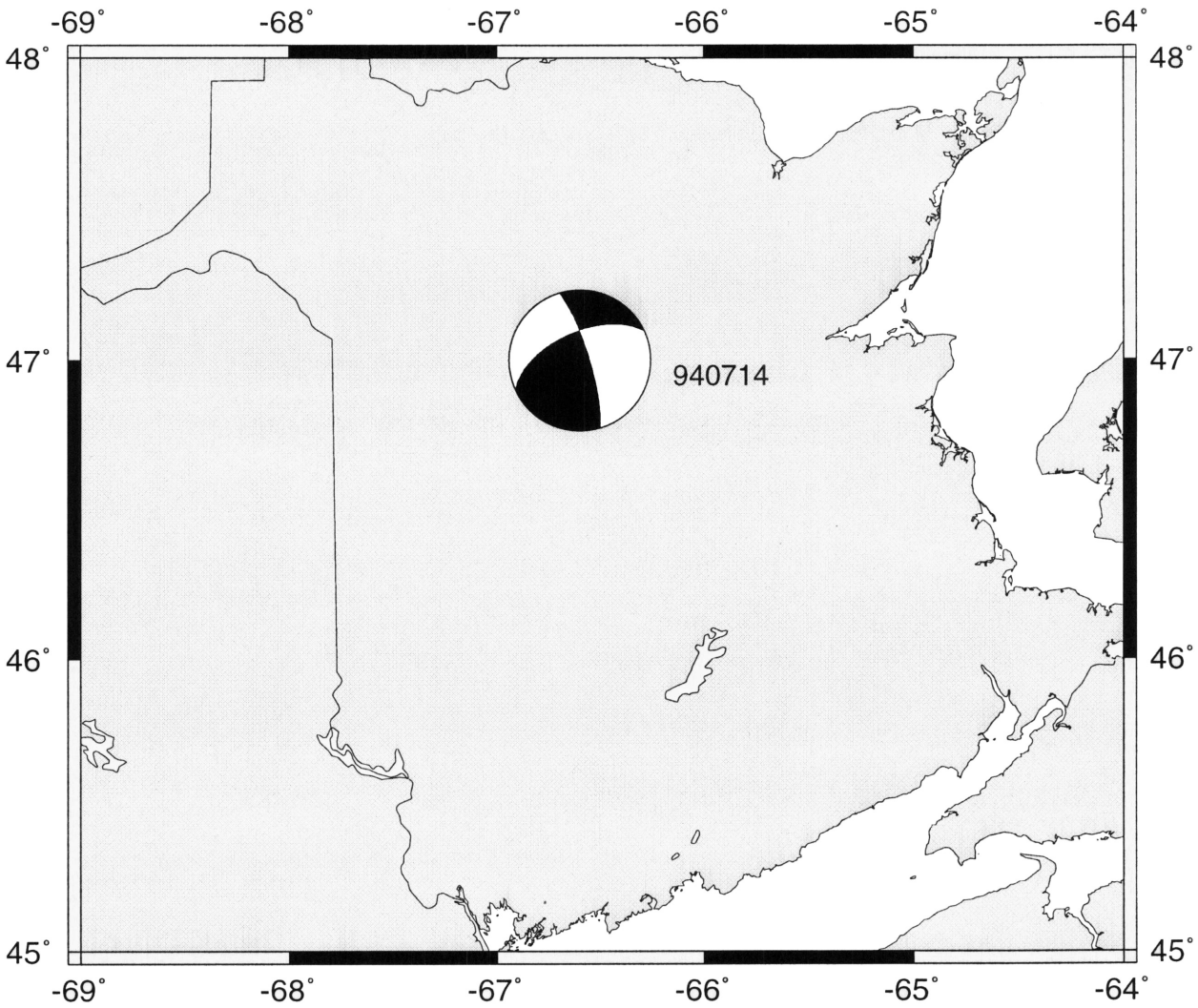

Figure 24

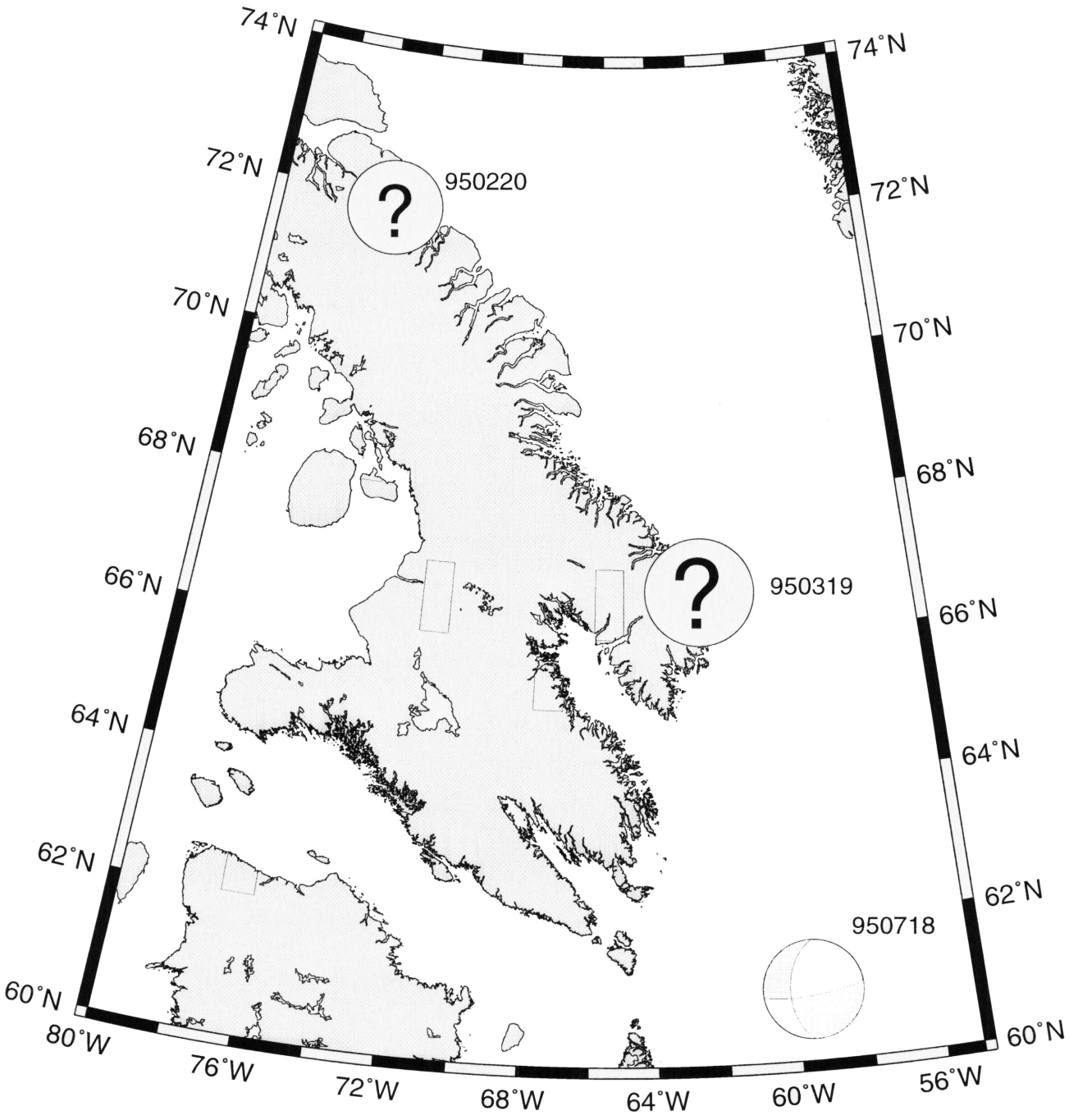
74°N
72°N
70°N
68°N
66°N
64°N
62°N
60°N
80°W
76°W
72°W
68°W
64°W
60°W
56°W
950220
950319
950718

Figure 25

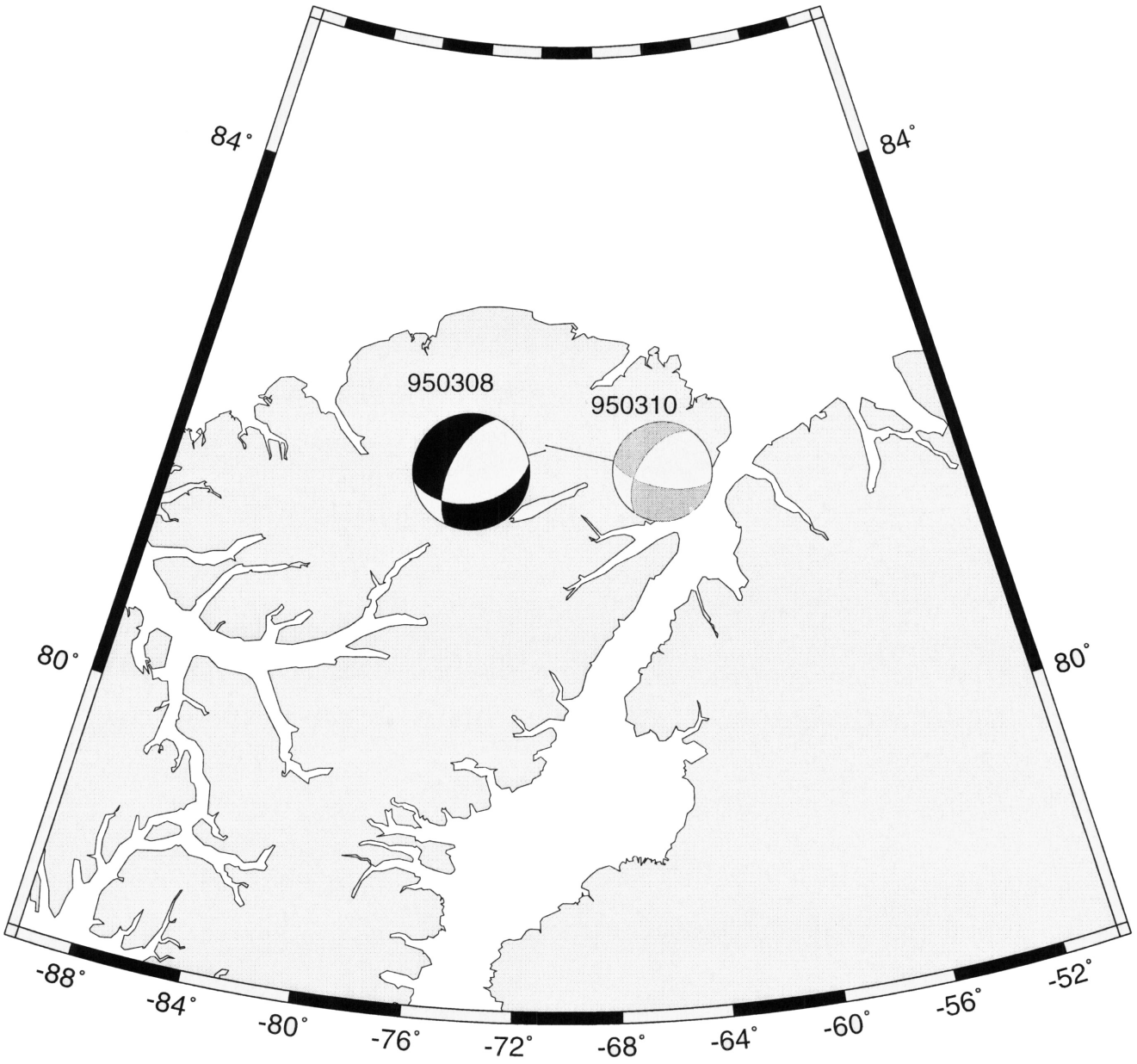

Figure 26

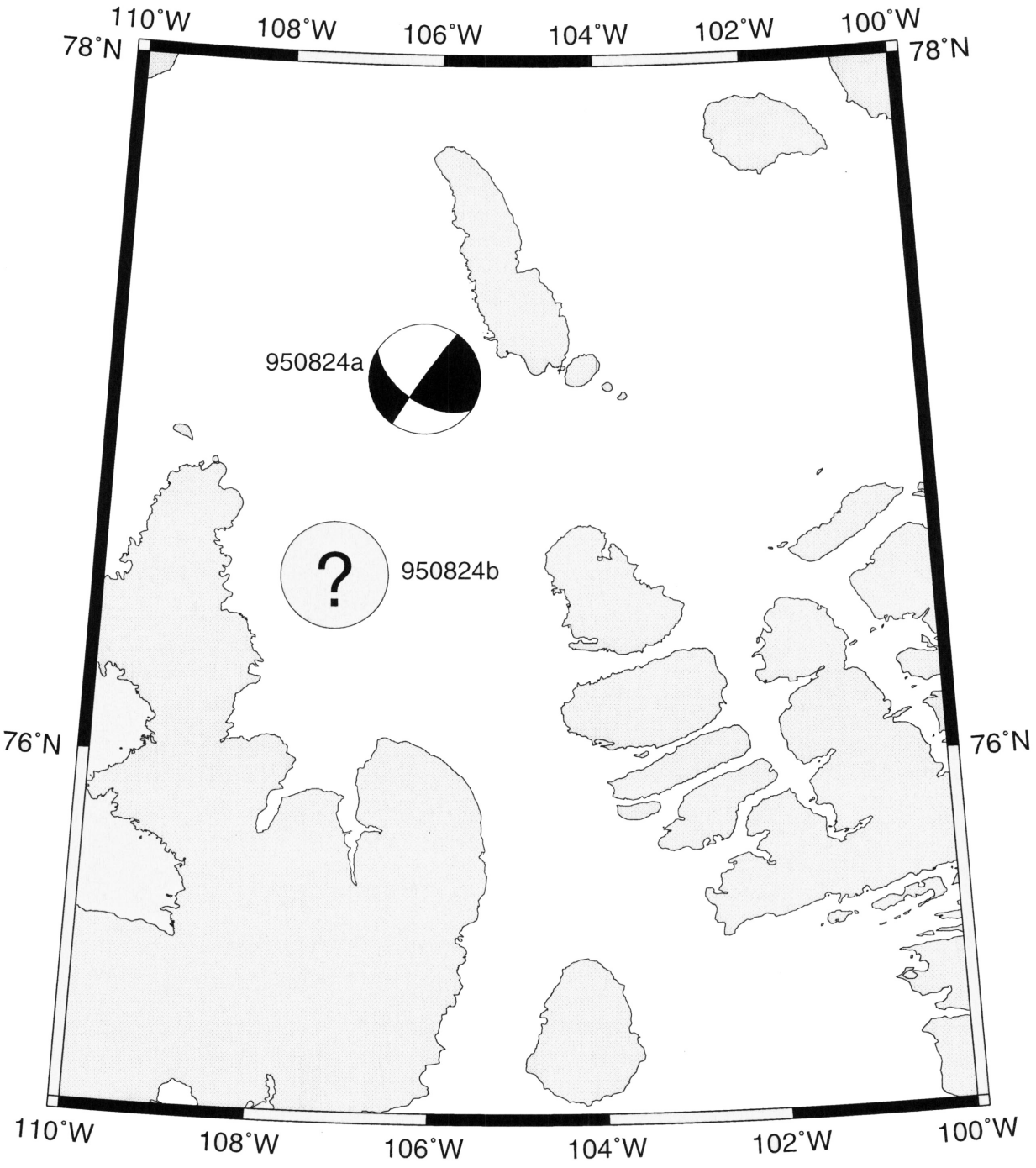

Figure 27

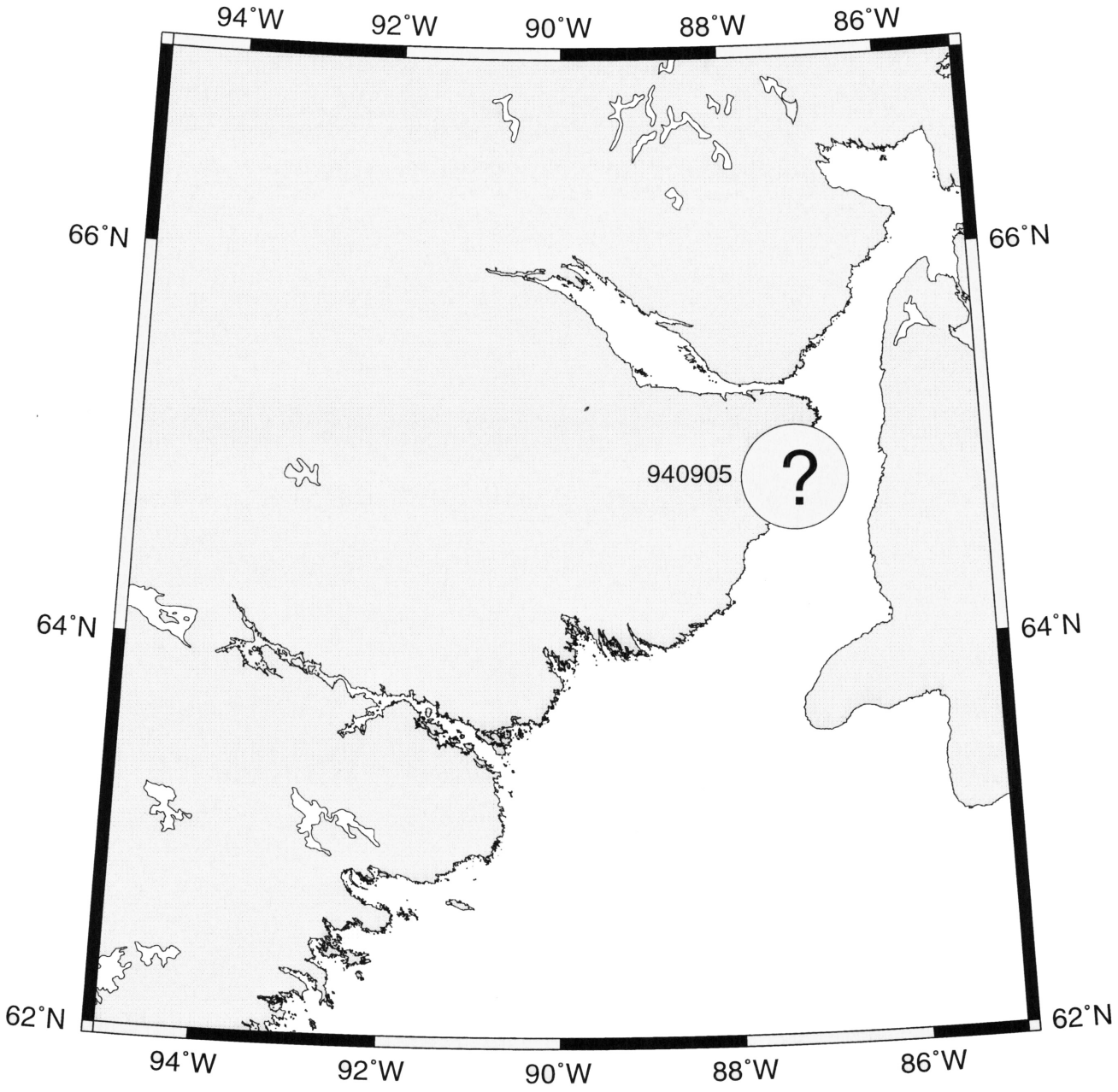

Figure 28

CONCLUSIONS

We have determined focal mechanisms for five of the ten earthquakes of magnitude 4.0 or greater that occurred in eastern Canada during 1994 and 1995. Some solutions are better constrained than others. One event had a previously published mechanism and therefore, we did not re-evaluate it. The four events for which focal mechanisms could not be determined occurred in offshore and northern regions where station density is low and azimuthal coverage is poor. We were also able to determine focal mechanisms for earthquakes in other remote regions, such as Ellesmere Island and the Byam Martin Channel. None of the focal mechanisms we determined was a surprise in terms of type of faulting. Combining the results of this study with several similar ones (Bent and Perry, 1999; Bent and Drysdale 2000, 2001) we can make several conclusions regarding the feasibility of determining focal mechanisms for eastern Canadian earthquakes. In the southeastern mainland regions (New Brunswick, southern Quebec, southeastern Ontario) it is almost always possible to determine a reasonably high quality mechanism for all events of magnitude 4.0 or greater. In the Laurentian Slope/Fan and Baffin Bay-Baffin Island regions station density is low and azimuthal coverage is poor. We could generally only determine mechanisms for earthquakes with magnitudes greater than 4.5. In some other regions, such as the Labrador Sea and the far north, station density is also low but the azimuthal coverage is somewhat better. We could obtain good quality A and B solutions for most of the larger earthquakes in these regions and solutions for some of the smaller earthquakes. The Boothia-Ungava seismic zone also has low station density but azimuthal coverage is reasonable if all stations are functioning properly. Again there is some correlation between magnitude and solution quality but it is possible to determine mechanisms for some of the smaller (magnitude 4.0-4.5) events.

ACKNOWLEDGMENTS

We thank our non-GSC colleagues who supplied us with waveforms and/or polarity information and Janet Drysdale for reviewing the manuscript.

TABLE
SUMMARY OF SOLUTIONS

	Plane 1				Plane 2				
Event	Strike(°)	Dip (°)	Rake (°)	Type*	Strike(°)	Dip (°)	Rake (°)	Type	Quality
940714	343	79	33	OT	246	57	167	SS	A
940905	??	??	??	??	??	??	??	??	N/A
940925	37	56	90	T	217	34	90	T	A**
950220	??	??	??	??	??	??	??	??	N/A
950308	80	45	–45	ON	145	46	–166	SS	A
950310	100	64	–44	ON	213	51	–146	ON	C
950319	??	??	??	SS or OT	??	??	??	SS or OT	B
950718	74	80	-39	ON	172	52	-168	SS	C
950824a	215	87	35	OT	123	55	177	SS	B
950824b	??	??	??	Not N	??	??	??	Not N	N/A

* SS = strike-slip (rake within 30° of pure strike-slip)
T = thrust (rake within 30° of pure thrust)
N = normal (rake within 30° of pure normal)
O = oblique (rake more than 30° from end member; ON = oblique-normal; OT = oblique thrust)

** solution and quality as stated in Lamontagne (1998)

REFERENCES

Adams, J. (1995). The Canadian crustal stress database: A compilation to 1994, *Geol. Surv. Canada Open File 3122*, 38 pp.

Basham, P. W., D. H. Weichert, F. M. Anglin and M. J. Berry (1982). New probabilistic strong seismic ground motion maps of Canada: A compilation of earthquakes source zones, methods and results, *Earth Physics Branch Open File 82-33*, 205 pp.

Bent, A. L. and H. S. Hasegawa (1992). Earthquakes along the northwestern boundary of the Labrador Sea, *Seism. Res. Lett.*, **63**, 587-602.

Bent, A. L. and C. Perry (1999). Focal mechanisms for eastern Canadian earthquakes: 1 January 1996- 30 June 1998, *Geol. Surv. Canada Open File 3698*, 148 pp.

Bent, A. L. and J. Drysdale (2000). Focal mechanisms for eastern Canadian earthquakes: 1 July 1998- 31 December 1998, *Geol. Surv. Canada Open File* 3870, 89 pp.

Bent, A. L. and J. Drysdale (2001). Focal mechanisms for eastern Canadian earthquakes of 1999, *Geol. Surv. Canada Open File* 4085, 107 pp..

Choy, G. L., J. Boatwright, J. W. Dewey and S. A. Sipkin (1983). A teleseismic analysis of the New Brunswick earthquake of January 9, 1982, *J. Geophys. Res.*, **88**, 2199-2212.

Hasegawa, H. S. (1977). Focal parameters of four Sverdrup Basin, Arctic Canada earthquakes in November and December of 1972, *Can. J. Earth Sci.*, **79**, 5458-5468.

Lamontagne, M. (1998). New and revised earthquake focal mechanisms of the Charlevoix seismic zone, Canada, *GSC Open File 3556*, 302 pp.

Snoke, J. A., J. W. Munsey, A. G. Teague and G. A. Bollinger (1984). A program for focal mechanism determination by combined use of polarity and SV-P amplitude data (abstract), *Earthquake Notes*, **55 (3)**, 15.

Tapley, W. C. and J. E. Tull (1991). SAC- Seismic Analysis Code Revision 4, Lawrence Livermore National Laboratory, Livermore, California, non-paginated.

Wetmiller, R. J., J. Adams, F. M. Anglin, H. S. Hasegawa and A. E. Stevens (1984). Aftershock sequences of the 1982 Miramichi, New Brunswick earthquake, *Bull. Seism. Soc. Am.*, **74**, 621-654.